NTNU – Trondheim
Norwegian University of
Science and Technology

Multivariate analysis of heat transfer and pressure drop in finned tube bundles

Tor Gunnar Fjelde Feten

Master of Energy and Environmental Engineering
Submission date: June 2013
Supervisor: Erling Næss, EPT
Co-supervisor: Anna Holfeld, EPT

Norwegian University of Science and Technology
Department of Energy and Process Engineering

NTNU
Norwegian University of Science and Technology

Department of Energy and Process Engineering

EPT-M-2013-37

MASTER THESIS

for

Stud.techn. Tor Gunnar Fjelde Feten

Spring 2013

Multivariate analysis of heat transfer and pressure drop in finned tube bundles

Multivariabel analyse av trykkfall og varmeovergang i finnede rørsatser

Background and objective

Exhaust gas from a gas turbine contains a large amount of heat that can be utilized for process purposes or for power generation. On offshore platforms, it is necessary to make heat recovery units as compact and light weight as possible. The department, in cooperation with SINTEF Energy Research and international oil companies engaged in a work which seeks to develop compact heat exchangers for heat recovery from exhaust gas from gas turbines. In the present project, finned tubes shall be considered. Existing correlations for heat transfer and pressure drop of finned tube bundles have limited validity ranges. Data from various experimenters shall be used to establish new correlations with a wider range of validity. A test rig for measurements on heat transfer and pressure drop on finned tube bundles is available in the laboratory of NTNU.

The following tasks are to be considered:

1. The method of multivariate analysis shall be described, and a suitable procedure for the analysis of the available heat transfer and pressure drop data shall be proposed.
2. Perform a multivariate analysis on the collected experimental data of solid and serrated finned tubes having staggered tube arrangements. The resulting correlations of heat transfer and pressure drop shall be presented, discussed and compared to available data and correlations. A sensitivity analysis shall be performed. Based on the results, additional experiments needed to improve the prediction accuracy and validity range shall be proposed.
3. Suggestions for further work shall be made.

Within 14 days of receiving the written text on the master thesis, the candidate shall submit a research plan for his project to the department.

When the thesis is evaluated, emphasis is put on processing of the results, and that they are presented in tabular and/or graphic form in a clear manner, and that they are analyzed carefully.

The thesis should be formulated as a research report with summary both in English and Norwegian, conclusion, literature references, table of contents etc. During the preparation of the text, the candidate should make an effort to produce a well-structured and easily readable report. In order to ease the evaluation of the thesis, it is important that the cross-references are correct. In the making of the report, strong emphasis should be placed on both a thorough discussion of the results and an orderly presentation.

The candidate is requested to initiate and keep close contact with his/her academic supervisor(s) throughout the working period. The candidate must follow the rules and regulations of NTNU as well as passive directions given by the Department of Energy and Process Engineering.

Risk assessment of the candidate's work shall be carried out according to the department's procedures. The risk assessment must be documented and included as part of the final report. Events related to the candidate's work adversely affecting the health, safety or security, must be documented and included as part of the final report. If the documentation on risk assessment represents a large number of pages, the full version is to be submitted electronically to the supervisor and an excerpt is included in the report.

Pursuant to "Regulations concerning the supplementary provisions to the technology study program/Master of Science" at NTNU §20, the Department res erves the permission to utilize all the results and data for teaching and research purposes as well as in future publications.

The final report is to be submitted digitally in DAIM. An executive summary of the thesis including title, student's name, supervisor's name, year, department name, and NTNU's logo and name, shall be submitted to the department as a separate pdf file. Based on an agreement with the supervisor, the final report and other material and documents may be given to the supervisor in digital format.

X Work to be done in lab (Water power lab, Fluids engineering lab, Thermal engineering lab)

☐ Field work

Department of Energy and Process Engineering, 16. January 2013

Olav Bolland
Department Head

Erling Næss
Academic Supervisor

Research Advisor: PhD student Anna Holfeld, NTNU

Preface

The project, Multivariate analysis of heat transfer and pressure drop in finned tube bundles, is written as master thesis at NTNU Gløshaugen. The project comprises 30 credits in the 10th semester of the master degree at the Department of Energy and Process Engineering.

I would like to thank my supervisor Erling Næss for all the feedback and advices during our meetings. I would also like to thank my co-supervisor Anna Holfeld for always being available and very helpful. Especially I am very grateful for all your feedback during the report writing process.

At last, I would like to thank my family for all your support during my time in Trondheim.

Trondheim, June 2013

Tor-Gunnar Fjelde Feten

Abstract

The exhaust gas from gas turbines contains a large amount of heat that can be utilized for process purposes or for further power generation. The heat recovery units on offshore platforms are required to be as compact and light as possible. During the design of waste heat recovery units correlations are used to estimate the heat transfer and pressure drop. The correlations in the literature have limited validity ranges. The aim of this project was to develop correlations with a wider range of validity than the correlations in the literature. Data from different experimenters, collected in databases, were used in order to establish the new correlations.

The report can be divided into the following two parts:

1) Literature survey of multivariate analysis:

A literature survey of the method of multivariate analysis was done. Here the aim was to find a method that could be used in order to develop the new correlations. The multivariate method called multiple linear regression was chosen. In order to select which variables to include in the multiple linear regression, the variable selection procedure called best subsets regression was carried out. The regression analysis was performed with the statistical software Minitab 16.

2) Regression analysis:

The data from the two available databases for serrated and solid fins were used in the regression analysis. Correlations for heat transfer and pressure drop were developed for both serrated and solid fins. It was decided to develop two different versions for each correlation: The first version was using different dimensionless groups for fin geometry, while the second version was using Ar (defined by PFR (1976)) as fin geometry effect. For both versions the effect of the Reynolds number and the tube bundle layout was included. In addition, the effect of the segment height on the heat transfer and the pressure drop was investigated.

Samandrag

Eksosgassen frå gassturbinar inneheld store mengder av varme som kan utnyttast til prosessformål eller til vidare kraftproduksjon. Det er eit krav om at varmegjenvinningseiningane på offshore plattformar er så kompakte og lette som mogleg. Under utforminga av einingar for varmegjenvinning av spelvarme blir korrelasjonar nytta til å estimere varmeovergangen og trykktapet. Korrelasjonane i litteraturen er gyldige for eit avgrensa område. Målet i dette prosjektet var å utvikle korrelasjonar som er gyldige for eit større område enn korrelasjonane i litteraturen. Data frå forskjellige eksperiment, samla i databasar, vart nytta for å utvikle dei nye korrelasjonane.

Rapporten kan delast inn i følgjande to delar:

1) Litteraturstudie av multivariabel analyse:

Eit litteraturstudie av metoden multivariabel analyse vart gjennomført. Her var målet å finne ein metode som kunne nyttast til å utvikle dei nye korrelasjonane. Den multivariable metoden kalla multippel lineær regresjon vart valt. For å velje kva variablar som skulle inkluderast i sjølve regresjonen vart ein seleksjonsprosedyre kalla best subsets regression nytta. Regresjonsanalysen vart gjennomført i det statistiske dataprogrammet Minitab 16.

2) Regresjonsanalysen:

Data frå dei to tilgjengelege databasane for serraterte og heiltrekte finner vart nytta i regresjonsanalysen. Korrelasjonar for varmeovergang og trykktap vart utvikla for både serraterte og heiltrekte finner. Det vart bestemt å utvikle to versjonar for kvar korrelasjon:

Den første versjonen brukte forskjellige dimensjonslause grupper for finnegeometri, medan den andre versjonen brukte Ar (definert av PFR (1976)) som finnegeometrieffekt. For begge versjonane vart også effekten av Reynoldstalet og røyrlayout inkludert. I tillegg vart effekten av segmenthøgda på varmeovergangen og trykktapet undersøkt.

Table of content

Nomenclature list

Symbol	Unit	Comment
A	m^2	Total heat transfer area
$A_{base\ tube}$	m^2/m	Base tube surface area per unit length
Ar	-	Ratio of the overall extended surface area to the area of the base tube.
$A_{segmented\ part,\ fin}$	m^2/m	Surface area of segmented part of the fin (for I-foot fins) per unit length
Ar_{sol}	-	Ar for serrated fins calculated as for solid fins (see appendix B)
$A_{solid\ part,\ fin}$	m^2/m	Surface area of solid part of the fin (for I-foot fins) per unit length
A_t	m^2	Outside surface area tube except fins
A_t'	m^2/m	Outside surface area tube except fins per unit length
C	-	Constant
C_p	-	Mallows C_p
c_p	J/kgK	Specific heat capacity
d	m	Diameter
d_e	m	Effective tube outside diameter, (d_e=d_o+2t for L-foot finned tubes)
d_f	m	Fin diameter
d_h	m	Hydraulic diameter
d_i	m	Tube inside diameter
d_o	m	Tube outside diameter
Eu	-	Euler number, $Eu=2\Delta p\rho/G^2N_l=2\Delta p/\rho u_{max}^2N_l$
F	-	F-value (for F-test)
F_d	m^2/m	Twice the free-flow area in diagonal plane between two tubes
F_t	m^2/m	Free-flow area in transversal plane between two tubes
G	Kg/m^2s	Mass flux in narrowest free-flow area
h	$W/(m^2K)$	Heat transfer coefficient
h_e	m	Effective fin height (h_e=h_f-t for L-foot fins)
h_f	m	Fin height
h_s	m	Segment height of fin (for I-foot fins)
k	W/(mK)	Thermal conductivity
k	-	Number of predictors in the regression model

MSE	-	Mean square error
MS_{reg}	-	Mean square regression
n	-	Number of observations
N_f	1/m	Number of fins per meter
N_l	-	Number of tube rows in direction of flow
Nu	-	Nusselt number, $Nu=hd_e/k$
Δp	Pa	Pressure drop
P_l	m	Longitudinal tube pitch
Pr	-	Prandtl number, $Pr=c_p\mu/k$
P_t	m	Transversal tube pitch
P_x	m	Diagonal tube pitch
R^2	-	Ratio between the explained variation in the dependent variable y and the total variation in y ($R^2=SS_{reg}/SS_{tot}$)
R_{adj}^2	-	The adjusted R^2
Re	-	Reynolds number, $Re=\rho u_{max}d_e/\mu$
Re_{df}		$Re_{df}=\rho u_{max}d_f/\mu$
Re_{dh}	-	$Re_{dh}=\rho u_{max}d_h/\mu$
P	-	P-value
s	m	Fin spacing, $s=s_f-t$
S	-	$\sqrt{MSE}$, square root of the mean square error.
s_f	m	Fin pitch
SS_{reg}	-	Components explained or accounted for by the regression line
SS_{res}	-	Components unexplained (sum of squared residuals)
SS_{tot}	-	Total variation in y ($SS_{tot}=SS_{reg}+SS_{res}$)
t	m	Fin thickness
t	-	t-value
T	K	Temperature
T_b	K	Average or bulk gas temperature
T_s	K	Average fin surface temperature
t_w	m	Tube wall thickness
u	m/s	Velocity
u_{max}	m/s	Velocity of air at minimum cross section
VIF	-	Variance inflation factor

w_f	m	Fin segment width

Greek letters:

Symbol	Unit	Comment
β	°	Tube layout angle (figure 2)
β	-	Beta coefficient
μ	kg/(ms)	Kinematic viscosity
ρ	kg/m^3	Density

Subscripts:

adj	Adjusted
b	Bulk
d_h	Based on hydraulic diameter as length scale
d_f	Based on fin diameter as length scale
e	Effective
f	Fin
h	Hydraulic
i	Inner
max	Maximum
o	Outer
reg	Regression
res	Residuals
s	Surface
t	Tube
tot	Total
w	Wall
∞	Infinite

List of figures

List of tables

1 Introduction

1.1 Background

Finned tube bundles are used both for waste heat recovery and steam production. Gas turbines are widely used offshore for power generation. The exhaust gas from gas turbines contains a large amount of heat that can be utilized for process purposes or for further power generation. The heat recovery units on offshore platforms are required to be as compact and light weight as possible. The Department of Energy and Process Engineering cooperates with Sintef Energy Research and international oil companies in order to develop compact heat exchangers for heat recovery from exhaust gas from gas turbines. The heat recovery units arranged as finned tube bundles shall be considered in the present project.

During the design of a waste heat recovery unit (WHRU) correlations are used to estimate the heat transfer and pressure drop. The correlations developed by the different authors for heat transfer and pressure drop for finned tube bundles have limited validity ranges. Therefore data from different experimenters, collected in databases, shall be used to establish new correlations with a wider range of validity.

1.2 Structure of the report

Chapter 2 gives an overview over multivariate analysis. Here the multivariate analysis is explained in general and more specifically. Also the results from a literature survey of methods used in earlier reports are presented. Further the multivariate method multiple linear regression is described in detail as this method was chosen for the data analysis. The different techniques for multiple linear regression are described, because the choice of technique is important for the variable selection procedure.

In chapter 3 the results from the regression analysis are presented. The results from the analysis of the heat transfer data and pressure drop data for serrated fins are presented in chapter 3.4.2. The results from the analysis of the same data for solid fins are presented in chapter 3.4.3. The correlations developed in the analysis are compared with correlations from the literature in chapter 3.5. In chapter 3.6 a sensitivity analysis of the correlations presented in chapter 3.4 is performed. The results from an investigation of the impact of the segment height on the heat transfer and on the pressure drop are presented in chapter 3.7.

2 Multivariate analysis

2.1 General about multivariate analysis

According to Esbensen et al. (2002) most of the problems in the world are multivariate in nature, in other words there are many variables that contribute to them. It is very seldom that a property only depends on one variable. Multivariate analysis consists of a collection of methods that can be used when several measurements are made on each individual object in one or more samples. The measurements are usually referred to as variables, while the individuals or objects often are referred to as units or observations, Alvin (2002) .

Often it is necessary to observe, study or measure more than one variable simultaneously. If the measuring correspond directly to the phenomenon being investigated everything is fine, Esbensen et al. (2002). For example, using a temperature sensor to measure a temperature is possible. When a desired parameter cannot be measured directly, it is necessary to turn to indirect observations, Esbensen et al. (2002). This means that something else needs to be measured to determine what one really wants to know. An example is when the aim is to measure the heat transfer coefficient: Here indirect observations as temperature and flow rate are measured in order to find the heat transfer coefficient.

The aim of this project is to find how different parameters affect the heat transfer and the pressure drop in finned tube bundles. Neither the heat transfer nor the pressure drop depends on one single parameter. The combination of different geometrical parameters determines the heat transfer and the pressure drop. Therefore a multivariate analysis should be performed. Here the different parameters for the flow, the fin geometry and the tube bundle layout will be the variables, while the heat transfer (On dimensionless form, $NuPr^{-1/3}$) and the pressure drop (On dimensionless form, Eu) will be the observations in the respective analysis.

2.2 Methods of multivariate analysis

Esbensen et al. (2002) divide multivariate analysis into three main groups:

1) Data description

According to Esbensen et al. (2002) a large part of multivariate analysis is concerned with simply "looking" at the data. The aim of the data description could be different things, for example to determine means, standard deviations or correlation. For example to find the correlation between the heat transfer and the different parameters could be useful as this could give an impression of what to expect from the multivariate data analysis later on.

A common method for data description is Principal component analysis (PCA).

2) Discrimination and classification

According to Esbensen et al. (2002) discrimination separates groups of data. The method classifies observations into homogenous groups, for example sweet and sour apples.

Discriminant analysis is a common method for discrimination.

Classification has a similar purpose as discrimination, but according to Esbensen et al. (2002) here one typically knows the relevant groupings in the data set before the analysis.

3) Regression and prediction

Regression is an approach to relate two sets of variables to each other. This means to determine one (eventually several) y-variables on the basis of a set of relevant x-variables.

There are different regression methods. Examples are Principal Component Regression (PCR), Partial Least Squares Regression (PLS-R) and Multiple Linear Regression (MLR).

Prediction means to determine y-values for the new x-objects, based on a previously estimated x-y model, Esbensen et al. (2002). For example to predict $NuPr^{-1/3}$ for a completely new geometry by using a correlation developed earlier.

2.3 Methods used in the literature

In order to find a suitable procedure for the analysis of the available heat transfer and pressure drop data, a literature study was done searching for the methods other authors had used. In most of the reports it was only mentioned that multiple linear regression was used, but Briggs and Young (1963) described their method more specific:

They found the dimensions that could be important in describing the tube and tube layout (h_f, s, t, d_o and d_f). The dimensions were further arbitrarily arranged into dimensionless groups $\left(\frac{s}{t}, \frac{t}{d_o}, \ldots\right)$. As many parameters as possible were considered in order to prevent the exclusion of any significant parameters.

A step-by-step regression analysis of the data was made, and an F level (See chapter 3.1 for definition) of 3,95 was used for removing any parameters which was not significant. For the number of data an F level=3,95 indicated that the parameter under question had a probability of 95 % of being significant to the correlation. The computer program they used selected the dimensionless groups with the largest range of values as the first variable to be tried. If the F level of the variable was greater than 3,95, the variable was included in the correlation. After the first dimensionless group had been considered, the computer then selected from the remaining groups the one with the largest range of values and repeated the process. This step-by-step regression analysis was continued until all the variables had been considered. In other words a forward selection (See chapter 2.4.1.1) method was used.

Næss (2007) also described the regression method he used in detail. The dimensionless heat transfer coefficient was expressed as:

$$Nu = f_1(geometry) \cdot f_2\left(Re_{d_f}\right) \cdot Pr^{1/3} \qquad (1)$$

The influence of the Reynolds number was first studied, and the relation between $NuPr^{-1/3}$ and Re was observed to follow simple power-law dependencies (See equation below):

$$Nu = C_1 \cdot Re^m \cdot Pr^{1/3} \qquad (2)$$

The individual exponents m were evaluated by a linear least squares regression analysis.

The individual geometry specific constants C_1 were calculated using the equation below:

$$C_1 = \frac{1}{n} \cdot \sum_{i=1}^{n} \frac{Nu_i \cdot Pr^{-1/3}}{{Re_i}^m} \tag{3}$$

The average value of m, $\overline{m}$, was used in the equation above.

In order to explore the impact of the geometry, several dimensionless groups (d_f/d_e, P_t/d_e etc.) were constructed and fitted to the data assuming simple power-law dependencies. Parameters cancelling each other and parameters with unrealistically high or low exponents were removed. Parameters not contributing significantly to the improvement of the correlation accuracy were also discarded. Following this procedure the heat transfer equation had the general form:

$$Nu = C_1 \cdot {Re_{d_f}}^m \cdot Pr^{1/3} \cdot f_1(Tube\ layout) \cdot f_2(Fin\ geometry) \tag{4}$$

The same method was used for the pressure drop data, resulting in the general equation for the Euler number:

$$Eu = C_2 \cdot \left[C_3 + \frac{C_4}{Re^n}\right] \cdot f_3(Tube\ layout) \cdot f_4(Fin\ geometry) \tag{5}$$

The method used by Næss (2007) also seems like a stepwise method, as several different parameters are included and removed if they are not significant (Backward elimination).

Conclusion: The literature survey gave the impression that multiple linear regression was the common method to analyze the experimental heat transfer and pressure drop data. Therefore it was chosen to use this method also in this project.

2.4 Multiple linear regression

Multiple linear regression is a general statistical technique through which one can analyze the relationship between a dependent or criterion variable and a set of independent or predictor variables. According to Kasai (1998) multiple linear regression may be viewed either as a descriptive tool by which the linear dependence of one variable on others is summarized and decomposed, or as an inferential tool by which the relationships in the population are evaluated from the examination of sample data.

Usually the response variable is denoted by y and the set of predictor variables by x_1, x_2,x_3,…, x_k, where k denotes the number of predictor variables. The true relationship between y and x_1, x_2,x_3,…, x_k can be approximated by the regression model, Chatterjee and Hadi (2006):

$$y = f(x_1, x_2, \dots, x_k) + \varepsilon \tag{6}$$

where ε is assumed to be a random error representing the discrepancy in the approximation.

An example of the relationship between y and x_1, x_2,x_3,…, x_k is the linear regression model:

$$y = \beta_0 + \beta_1 \cdot x_1 + \beta_2 \cdot x_2 + \cdots + \beta_k \cdot x_k + \varepsilon \tag{7}$$

where β_0, $\beta_{1,\dots,}$ β_k are called the regression coefficients or parameters, are unknown constants to be determined from the data. The regression coefficient, for example β_1, stands for the change in y with a change of one unit in x_1 when the other variables x_2,…,x_k are held constant or controlled for. The estimated regression equation becomes:

$$\hat{y} = \hat{\beta}_0 + \hat{\beta}_1 \cdot x_1 + \hat{\beta}_2 \cdot x_2 + \cdots + \hat{\beta}_k \cdot x_k + \varepsilon \tag{8}$$

A hat on top of a parameter denotes an estimate of the parameter. The value ŷ is called the fitted value, Chatterjee and Hadi (2006). Using equation 8, one can compute n fitted values one for each of the n observations in the data. For example, the fitted ith value would be:

$$\hat{y}_i = \hat{\beta}_0 + \hat{\beta}_1 \cdot x_{i1} + \hat{\beta}_2 \cdot x_{i2} + \cdots + \hat{\beta}_k \cdot x_{ik} + \varepsilon \tag{9}$$

The total sum of squares in y is the variability of the dependent variable y. According to Walpole et al. (2007) this can be partitioned into components which are:

1) Components that are explained or accounted for by the regression line (regression sum of squares), denoted by SS_{reg} which is defined in equation 10.
2) Components that are unexplained (the sum of squared residuals), SS_{res}, defined in equation 11.

$$SS_{reg} = \sum (\hat{y} - \bar{y})^2 \tag{10}$$

$$SS_{res} = \sum (y - \hat{y})^2 \tag{11}$$

The total variation in y can then be defined as:

$$\begin{gathered} SS_{tot} = SS_{reg} + SS_{res} \\ SS_{tot} = \sum (\hat{y} - \bar{y})^2 + \sum (y - \hat{y})^2 \end{gathered} \tag{12}$$

When this portioning is given, a measure of prediction accuracy and the strength of linear association is the ratio between the explained variation in the dependent variable y and the total variation in y:

$$R^2 = \frac{SS_{reg}}{SS_{tot}} = \frac{SS_{tot} - SS_{res}}{SS_{tot}} \tag{13}$$

The adjusted R^2 or adjusted multiple coefficient of determination is defined as:

$$R_{adj}{}^2 = 1 - \frac{SS_{res}/(n-k-1)}{SS_{tot}/(n-1)} \tag{14}$$

Walpole et al. (2007) point out that the adjusted R^2 is a variation on R^2 that provides an adjustment for degrees of freedom. This term cannot decrease as terms are added to the model. In other words, R^2 does not decrease as the error degrees of freedom n-k-1 are reduced, the latter result being produced by an increase in k, the number of model terms, Walpole et al. (2007).

2.4.1 Multiple linear regression techniques

Multiple linear regression can be performed with different techniques. In the next sections two of the most common multiple regression techniques are presented:

2.4.1.1 Stepwise regression

One standard procedure for searching for the "optimum subset" of variables in the absence of orthogonality is a technique called stepwise regression, Walpole et al. (2007). This is based on the procedure of sequentially introducing the variables into the model one at a time.

One way to select variables is to use the method called forward selection. In the forward selection procedure the variables are inserted one at a time until a satisfactory regression equation is found. Walpole et al. (2007) suggest the following procedure:

Step 1: Choose the variable that gives the largest SS_{reg} when performing a simple linear regression with y or, equivalently, that which gives the largest value of R^2. This initial variable is called x_1.

Step 2: Choose the variable that when inserted in the model gives the largest increase in R^2, in the presence of x_1, over the R^2 found in step 1. This is the variable x_p for which

$$R(\beta_p|\beta_1) = R(\beta_1|\beta_p) - R(\beta_1) \tag{15}$$

is largest. This variable is called x_2. The regression model with x_1 and x_2 is then fitted and R^2 observed.

This process is continued until the most recent variable inserted fails to induce a significant increase in the explained regression. Such an increase can be determined at each step using the appropriate F-test or t-test. For example in step 2 the value

$$F = \frac{R(\beta_2|\beta_1)}{S^2} \tag{16}$$

can be used to test the appropriateness of x_2 in the model. Here the value of S^2 is the mean square error (MSE) for the model containing the variable x_1 and x_2. If $F < F\alpha(1,n\text{-}3)$ at step 2 for a prechosen significance level (often α=0,05 is chosen), x_2 is not included and the process is terminated, resulting in a simple linear equation relating y and x_1. However, if $F > F\alpha(1,n\text{-}3)$, one can proceed to the next step and try to add more variables.

Backward elimination involves the same concept as forward selection except that one begins with all the variables in the model, Walpole et al. (2007). Walpole et al. (2007) present an example where five variables are under consideration. The procedure is as follows:

Step 1: Fit a regression equation with all five variables included in the model. Choose the variable that gives the smallest value of the regression sum of squares adjusted for the others. Suppose that this variable is x_2. Remove x_2 from the model if

$$F = \frac{R(\beta_2|\beta_1,\beta_3,\beta_4,\beta_5)}{S^2} \tag{17}$$

is insignificant (If $F < F_\alpha$). If one of the variables is removed in step 1, perform the regression with the remaining variables and repeat step 1.This process is repeated until the variable with the smallest adjusted regression sum of squares results in a significant F-value for some predetermined significance level (In other words until $F > F_\alpha$).

Stepwise regression is accomplished with a slight but important modification of forward selection procedure. The modification involves further testing at each stage to ensure the continued effectiveness of variables that had been inserted into the model at an earlier stage, Walpole et al. (2007). This is an improvement of forward selection because variables are both inserted and deleted. In the forward selection method none of the variables from the earlier stages are removed. When the stepwise regression is performed and a new variable has been entered into the regression equation through a significant increase in R^2 as determined by the F-test, all the variables already in the model are subjected to F-tests in light of this new variable and are deleted if they do not display a significant F-value. The procedure is continued until no additional variables can be inserted or deleted, Walpole et al. (2007).

2.4.1.2 Best subsets regression

The best subsets regression procedure (also called all possible subsets regression) is a common procedure when doing multiple regressions. This method goes beyond stepwise regression and tests all possible subsets of the set of potential independent variables.

According to Minitab's Statguide (Minitab version 16, 2010) the general method is to select the smallest subset that fulfills certain statistical criteria. The reason that one would use a subset of variables rather than a full set is because the subset model may actually estimate the regression coefficients and predict future responses with smaller variance than the full model using all predictors.

The best subsets regression procedure involves the following steps:

Step 1: First all the possible regression models derived from all the possible combinations of the candidate predictors (this can be a very large number of possible models).

As an example, when there are three candidate predictors x_1, x_2 and x_3, there are eight possible regression models that can be considered:

- The one model with no predictors
- The three models with only one predictor each; the model with x_1 alone, the model with x_2 alone and the model with x_3 alone.
- The three models with two predictors each; the model with x_1 and x_2, the model with x_1 and x_3 and the model with x_2 and x_3.

- And the one model with all three predictors; the model with x_1, x_2 and x_3.

In general, if there are k possible predictors, then there are 2^k possible regression models containing the predictors. So for many predictors there will be a lot of models to consider, but statistical software like Minitab manages to do this work.

Step 2: From the possible models identified in the first step, determine the one-predictor models that do the best at meeting some criteria, the two-predictor models that do the best and so on. When this is done, the number of possible regression models to consider is reduced. In order to pick the best models; the following criteria can be used:

1) The model with the largest R^2

2) The model with the largest adjusted R^2, R_{adj}^2.

3) The model with the smallest MSE (Mean square error), or $S = \sqrt{MSE}$.

$$MSE = \frac{SS_{res}}{n-k-1} = \frac{\sum(y-\hat{y})^2}{n-k-1} \qquad (18)$$

4) The model with the smallest Mallows C_p. The Minitab's Statguide gives this advice: Look for models where Mallows C_p is small and close to the number of predictors in the model plus the constant (p=k+1). A small Mallows C_p value indicates that the model is relatively precise (has small variance) in estimating the true regression coefficients and predicting future responses. Models with considerable lack-of-fit and bias have values of Mallows C_p larger than p. According to the Statguide of Minitab the Mallows C_p is calculated the following way:

$$C_p = \frac{SS_{res,p}}{MSE_m} - (n-2p) \qquad (19)$$

where $SS_{res,p}$ is SS_{res} for the model under consideration, MSE_m is the mean square error for the model with all predictors included, n is the number of observations and p is the number of terms in the model, including the constant.

2.5 Choice of multiple linear regression method for the data

It seems like the stepwise regression method is the most commonly used regression method in the old reports. However, a meeting with a statistician gave the impression that the stepwise regression method was out of fashion and not recommended to use. Instead it was recommended to use the best subsets regression, because this tests all the possible variables at once and finds the best combination of the variables. Whittingham et al. (2006) also suggested that use of stepwise multiple regression was bad practice. The following principal drawbacks of stepwise multiple regression were presented:

1) Bias in parameter estimation

2) Inconsistencies among model selection algorithms

3) An inherent (but often overlooked) problem of multiple hypothesis testing

4) An inappropriate focus or reliance on a single best model

Best subsets regression tests all possible models and identifies the best-fitting regression models that can be constructed with the variables specified. It is an efficient way to reduce the amount of variables in the model. In addition, no variables are forgotten as all the possible combinations of variables are tested (All possible models with one variable, two variables and so on are tested).

The Statguide of Minitab (Minitab 16) gives the following general guideline when the choice is between best subsets regression and stepwise regression:

1) For data sets with a small number of predictors, best subsets regression is preferable to stepwise regression because it provides information on more models.

2) For data sets with a large number of predictors (>32 in Minitab), stepwise regression is preferable to best subsets regression because best subsets regression requires a significant amount of computational resources (which may not be available).

In the regression analysis the amount of variables would be quite much lower than 32. Therefore it was decided to use the best subsets regression method when working with the heat transfer and pressure drop data.

2.6 Software for the data analysis

The statistical software Minitab (version 16, 2010) has been used for the data analysis. Minitab can perform different multivariate methods, plot graphs, calculate basic statistics etc. Both best subsets regression and stepwise regression can be performed in the program. Especially the best subsets regression command is very useful as the program manages to find the best models when using several variables.

Another positive thing about Minitab is that data from Microsoft Excel can be copied directly into the program. The data for heat transfer and pressure drop are exported from the database program Filemaker Pro to Microsoft Excel. Further it is copied from Excel into Minitab.

3 Regression analysis

3.1 Test for significance

To test whether a significant relationship between the dependent variable and all the independent variables exists, the F-test could be used. The F-test is also referred to as the test for overall significance. Here the F-value must be calculated. The F-value is defined by the following ratio:

$$F = \frac{SS_{reg}/k}{SS_{res}/(n-k-1)} = \frac{R^2/k}{(1-R^2)/(n-k-1)} \tag{20}$$

F is then compared with the F-distribution, with three different parameters; k, n-k-1 and the significance level (typically 95 %), Esbensen et al. (2002). The F-value can be found in a statistical table. If F>F-value, then the effect is regarded to be significant, Esbensen et al. (2002).

A complementary measure is the P-value, Esbensen et al. (2002). The P-value is the probability that an independent variable has no effect on the dependent variable. If the P-value found is small, the effect is significant.

Usually, a hypothesis is formulated to test for overall significance as done by Walpole et al. (2007). Here the null hypothesis is that all the parameters are equal to zero, while the alternative hypothesis is that not all of the parameters are equal to zero:

H_0: $\beta_1=\beta_2=\ldots=\beta_k=0$

H_a: One or more slope terms is non-zero.

The rejection rule: For a certain value α (often 0, 05) and a certain degrees of freedom find F_α.

Reject H_0 if P-value≤α or F≥ $F_{\alpha.}$ When the regression analysis is performed in Minitab, the P-value is a part of the output.

The t-test on the other hand tests for individual significance, in other words it is used to find out whether each of the independent variables is significant. The t-value is used to perform the t-test. The t-value can be calculated the following way:

$$t = \frac{\hat{\beta}_i}{S_{\hat{\beta}_i}} \tag{21}$$

As for overall significance a hypothesis test is formulated. The null hypothesis is that the single parameter is equal to zero, while the alternative hypothesis is that the parameter is non-zero:

H_0: $\beta_i=0$

H_a: $\beta_i \neq 0$

The rejection rule: reject H_0 if P-value$\leq\alpha$ or if $t\leq -t_{\alpha/2}$ or $t\geq t_{\alpha/2}$ where $t_{\alpha/2}$ is based on a t-distribution with n-k-1 degrees of freedom.

3.2 Multicollinearity

When doing multiple regression analysis one should be aware of the possibility for multicollinearity in the regression model. According to Esbensen et al. (2002) collinearity means that the x-variables are intercorrelated to a non-neglectable degree, that the x-variables are linearly dependent to some degree; for example

$$x_1 = f(x_2, x_3, \dots, x_k)$$

Lee and Cincotta (2007) point out that multicollinearity affects the standard errors of estimated regression coefficients, biasing significance tests, the estimated regression coefficients themselves and possibly also forecasted values for the dependent variable, y.

In order to find out if there is collinearity in the model one can evaluate the term VIF (Variance inflation factor). VIF is the degree to which the variance β_i is increased because of the degree to which x_i is correlated with the other predictors, Lee and Cincotta (2007).

VIF can be evaluated the following way, Stine (1995):

$$VIF_k = \frac{1}{1 - {R_k}^2} \qquad (22)$$

where ${R_k}^2$ is the R^2 statistics when doing the regression with the variable x_k as the response and all the other variables as predictors (x-variables).

A rough rule of thumb is that variance inflation factor greater than 10 give some cause for concern, Der and Everitt (2012). Larose (2006) presents the following rule of thumb:

VIF≥5 indicates moderate multicollinearity, VIF≥10 indicates serious multicollinearity.

3.3 Description of the procedure chosen for the data analysis

In this section the method used when analyzing the heat transfer and pressure drop data will be described. There will also be examples of output and how to interpret the output:

As mentioned in the previous chapter it was decided to perform multiple linear regression analysis of the available data. The method can be divided into two different steps:

1) Performing the best subsets regression in order to do the selection of variables.

2) Perform the multiple linear regression using the variables selected from the best subsets regression.

After step two it is important to study the results of the regression analysis, including the beta-coefficients, R^2-value, P-values (See chapter 3.1) and variance inflation factor (See chapter 3.2).

As an example the output from the regression analysis for all the heat transfer data (except from the data from Cox (1973) and Schryber (1945), see chapter 3.4.1.2 for discussion) for serrated fins (for F_t/F_d<1,0) is presented below:

The data were $\log_{10}$-transformed before the regression as the aim was to get a correlation on the following form:

$$Nu \cdot Pr^{-1/3} = C_1 \cdot Re^a \cdot (Tube\ layout\ effect)^b \cdot (fin\ geometry\ effect)^c \tag{23}$$

$$\log\left(Nu \cdot Pr^{-1/3}\right) = log(C_1) + a \cdot log(Re) + \mathrm{b} \cdot \log\left(\frac{P_t}{P_l}\right) + c \cdot log\left(\frac{P_t}{d_e}\right) + d \cdot log\left(\frac{h_e}{s_f}\right) + \ e \ \cdot log\left(\frac{t}{s_f}\right) + f \cdot log\left(\frac{d_f}{d_e}\right) \tag{24}$$

The best subsets regression using the dimensionless groups in the equation above gave the following results:

Best Subsets Regression: logNuPr versus logRe; logPtPl; ...

```
Response is logNuPr
```

Vars	R-Sq	R-Sq(adj)	Mallows Cp	S	logRe	logPtPl	logPtde	logheff/sf	logdf/de	logt/sf
1	94,5	94,5	130,4	0,057590	X					
1	9,6	9,4	7310,2	0,23389		X				
2	95,1	95,1	81,0	0,054386	X			X		
2	94,9	94,8	103,2	0,055827	X					X
3	95,8	95,7	28,9	0,050767	X			X	X	
3	95,5	95,5	47,9	0,052096	X		X	X		
4	96,0	96,0	8,3	0,049207	X		X	X	X	
4	95,8	95,8	26,5	0,050524	X	X		X	X	
5	96,1	96,0	6,1	0,048974	X		X	X	X	X
5	96,0	96,0	10,3	0,049281	X	X	X	X	X	
6	96,1	96,0	7,0	0,048966	X	X	X	X	X	X

For five variables the R^2 reached its maximum and the value for Mallows Cp was the smallest one. S was also the lowest here. When the regression was performed with five variables, the dimensionless group t/s_f was found to be insignificant so therefore the regression was performed with four variables instead. Actually the R^2 did only increase with 0,1 % when including t/s_f, which was no significant increase in R^2. After the selection of variables through best subsets regression, the multiple linear regression (step 2) was performed. The output is presented below:

Regression Analysis: logNuPr versus logRe; logPtde; logheff/sf; logdf/de

```
The regression equation is
logNuPr = - 1,15 + 0,740 logRe + 0,236 logPtde - 0,206 logheff/sf
          + 0,507 logdf/de


Predictor        Coef   SE Coef       T      P    VIF
Constant     -1,15304   0,04873  -23,66  0,000
logRe        0,740438  0,008687   85,24  0,000  1,090
logPtde       0,23588   0,04979    4,74  0,000  1,229
logheff/sf   -0,20572   0,01970  -10,44  0,000  1,356
logdf/de      0,50728   0,07899    6,42  0,000  1,301


S = 0,0492073   R-Sq = 96,0%   R-Sq(adj) = 96,0%


Analysis of Variance

Source           DF       SS      MS        F      P
Regression        4  19,4764  4,8691  2010,90  0,000
Residual Error  332   0,8039  0,0024
Total           336  20,2803


Source      DF   Seq SS
logRe        1  19,1692
logPtde      1   0,0274
logheff/sf   1   0,1799
logdf/de     1   0,0999
```

Minitab displays the regression equation. In addition the standard error, the T-value, the P-value and the variance inflation factor (VIF) for each of the coefficients are displayed. In the analysis of variance table the degrees of freedom, SS_{reg}, SS_{res}, MS_{reg}, MSE, F-value and P-value for the model are presented. All the parameters are significant (P-value<0,05), the VIF is acceptable (no multicollinearity) and the R^2 is high.

At last the regression equation should be transformed:

$$Nu \cdot Pr^{-1/3} = 10^{-1,15304} \cdot Re^{0,7404} \cdot \left(\frac{h_e}{s_f}\right)^{-0,20572} \cdot \left(\frac{d_f}{d_e}\right)^{0,5073} \cdot \left(\frac{P_t}{d_e}\right)^{0,2359}$$

$$Nu \cdot Pr^{-1/3} = 0,0703 \cdot Re^{0,7404} \cdot \left(\frac{h_e}{s_f}\right)^{-0,20572} \cdot \left(\frac{d_f}{d_e}\right)^{0,5073} \cdot \left(\frac{P_t}{d_e}\right)^{0,2359} \quad (25)$$

3.4 Results from the regression analysis

3.4.1 Introduction

In the regression analysis for the heat transfer and pressure drop data for serrated fins, the data was divided into two parts:

1) The part of the data where the transversal free-flow area was the narrowest, in other words where $F_t/F_d<1,0$.

2) The part of the data where twice the diagonal free-flow area was the narrowest, $F_t/F_d>1,0$. This was only the case for some of the geometries from Næss (2007) (Geometry 3, 5, 7, 8, 9, 10 and 11).

This division was done to see how the effect of tube layout changed when the narrowest free flow area shifts from the transversal to the diagonal. Næss (2007) observed that the heat transfer coefficient increased with an increasing F_t/F_d up to a maximum at $F_t/F_d=1,0$. After that the heat transfer coefficient decreased monotonically.

For solid fins, there were only data for $F_t/F_d<1,0$. The data for both serrated and solid fins used in the analysis are for staggered tube layouts.

All the Minitab output from the regression analysis can be found in a separate attached file.

The data points for heat transfer in the databases are given as $NuPr^{-1/3}$, where the effective tube outside diameter is the length scale for Nu. The data points for pressure drop in the databases are given as the Euler number, where the velocity is taken at the narrowest cross-section. The Reynolds number is based on the effective tube outside diameter as length scale and the velocity in the narrowest cross-section.

The general form for the correlations for heat transfer and pressure drop respectively:

$$Nu \cdot Pr^{-1/3} = Constant \cdot Re^{m} \cdot f_1(Tube\ layout) \cdot f_2(Fin\ geometry) \tag{26}$$

$$Eu = Constant \cdot Re^{n} \cdot f_3(Tube\ layout) \cdot f_4(Fin\ geometry) \tag{27}$$

Different dimensionless groups for fin geometry and tube bundle layout were tried, and it was decided to develop two sets of equations:

One set where different dimensionless groups for fin geometry were used and one set where only one dimensionless group for fin geometry was used (Ar from PFR (1976)). Ar expresses the ratio of the overall extended surface area to the area of the base tube. The advantage of using Ar as dimensionless group for fin geometry is that the regression equation becomes simpler. However, the data from Kawaguchi et al. (2005)/Kawaguchi et al. (2006b) (for heat transfer) and Kawaguchi et al. (2004)/Kawaguchi et al. (2006a) (for pressure drop) could not be used when Ar was used as dimensionless group for fin geometry because the segment width for the serrated fins was not given in these papers. Ar was calculated the following way for serrated (L-foot and I-foot respectively) fins:

$$Ar = 1 + 2 \cdot N_f \cdot h_e \cdot \left(1 + \frac{t}{w_f}\right) \quad (28)$$

$$Ar = \frac{A_t' + A_{solid\,part,fin} + A_{segmented\,part,fin}}{A_{base\,tube}} \quad (29)$$

,where

$$A_t' = \pi \cdot d_o \cdot \left(1 - N_f \cdot t\right) \quad (30)$$

$$A_{solid\,part,fin} = \frac{\pi}{4} \cdot \left(\left(d_o + 2 \cdot \left(h_f - h_s\right)\right)^2 - {d_o}^2\right) \cdot 2 \cdot N_f \quad (31)$$

$$A_{segmented\,part,fin} = \left(2 \cdot h_s \cdot w_f + 2 \cdot h_s \cdot t + w_f \cdot t\right) \cdot \frac{\pi \cdot \left(d_o + 2 \cdot \left(h_f - h_s\right)\right)}{w_f} \cdot N_f \quad (32)$$

$$A_{base\,tube} = \pi \cdot d_o \quad (33)$$

For solid fins Ar was calculated using the equation below:

$$Ar = 1 + 2 \cdot N_f \cdot h_f \cdot \left(1 + \frac{h_f + t}{d_o}\right) \tag{34}$$

The figure below shows the difference between serrated and solid fins:

Figure 1 Tube with serrated fins (to the left) and tube with solid fins (to the right). (Delfintubes)

In the figures below the parameters for tube bundle layout and fin geometry are defined:

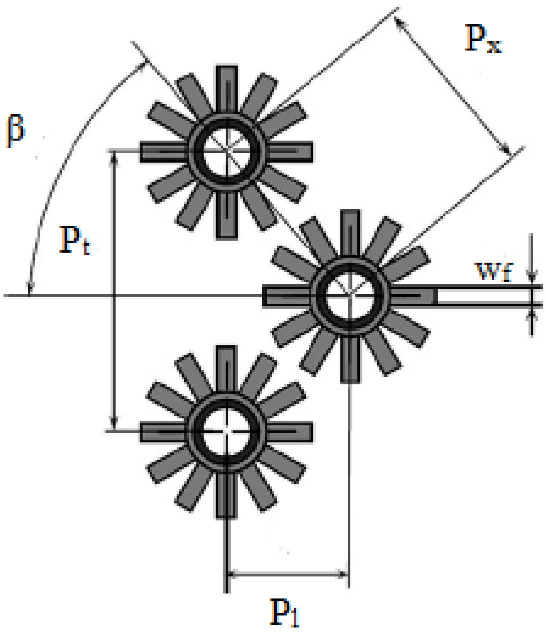

Figure 2 Tube bundle layout (staggered) (Næss (2010))

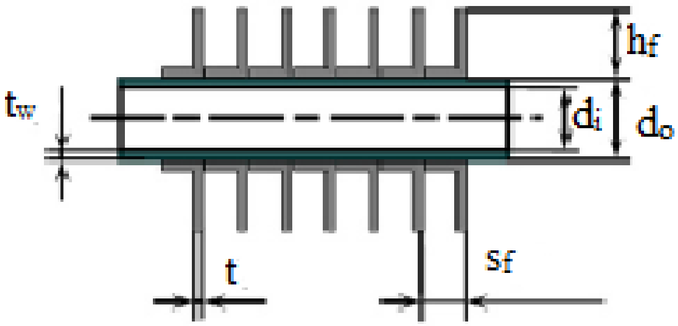

Figure 3 Fin geometry definitions (Næss (2010))

In the figure below the effective tube outside diameter and the effective fin height is defined for I-foot fins and L-foot fins respectively:

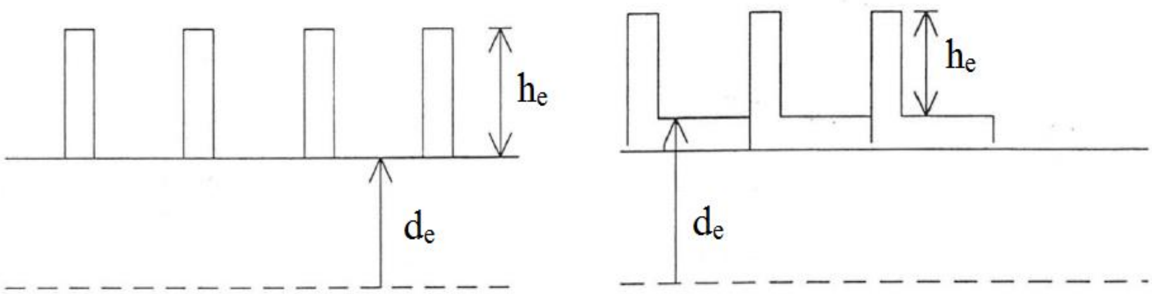

Figure 4 Effective tube outside diameter and effective fin height (Kaspersen (1995))

3.4.2 Serrated fins

3.4.2.1 The data

The data for heat transfer and pressure drop for serrated fins were taken out from a database implemented in the database program Filemaker Pro. The database was implemented by Kaspersen (1995). Heat transfer and pressure drop data from experiments after 1995 was added to the database by Feten (2012).

Table 1 Data sources for heat transfer and pressure drop data for serrated fins

	Data	**Fin type**
Schryber (1945)	Nu, Eu	L-foot
Worley and Ross (1960)	Nu, Eu	Stud fin tubes
Vampola (1966)	Nu, Eu	L-foot
Ackerman and Brunsvold (1970)	Nu, Eu	Stud fin tubes
Cox (1973)	Nu, Eu	Integral fins
Rabas and Eckels (1975)	Nu, Eu	L-foot
Weierman (1977)	Eu	I-foot
Weierman et al. (1978)	Nu, Eu	I-foot
Hashizume (1981)	Nu, Eu	I-foot
Kawaguchi et al. (2004)/Kawaguchi et al. (2005)/Kawaguchi et al. (2006a)/Kawaguchi et al. (2006b)	Nu, Eu	I-foot
Næss (2007)	Nu, Eu	L-foot
Hofmann (2009)	Nu, Eu	U-shaped
Ma et al. (2011)	Nu, Eu	I-foot

3.4.2.2 Heat transfer data

The regression analysis was first performed for all the heat transfer data for $F_t/F_d<1,0$. When the calculated and experimental values for $NuPr^{-1/3}$ were compared, it was observed that the data from Cox (1973) were calculated too low (ratio between calculated and experimental values ca. 0,7-0,85). Cox (1973) used integral fins in the experiments, so this could be the reason why the regression equation estimated these data too low. On the other hand the data from Schryber (1945) were estimated too high (ratio between calculated and experimental values ca. 1,2-1,45).

In order to get a more accurate regression equation for the rest of the heat transfer data, the data from Cox (1973) and Schryber (1945) were removed. After that the regression analysis was performed again.

The regression analysis gave the following regression equation for the heat transfer for serrated fins (the same equation as the one presented in the example in chapter 3.3):

$$Nu \cdot Pr^{-1/3} = 0{,}0703 \cdot Re^{0{,}7404} \cdot \left(\frac{P_t}{d_e}\right)^{0{,}2359} \cdot \left(\frac{h_e}{s_f}\right)^{-0{,}20572} \cdot \left(\frac{d_f}{d_e}\right)^{0{,}5073} \tag{25}$$

The exponent for the Reynolds number is rather high (0,7404) compared to the exponent in the correlation from Næss (2007). The reason could be that the large amount of data from Kawaguchi et al. (2006b) dominate in the regression analysis (the exponent for the Reynolds number in their correlation was 0,81). Also it is observed that the exponent for the ratio between the fin diameter and the effective tube outside diameter is almost the same as in the correlation from Weierman (presented in McKetta (1992)). In the figure below the calculated values using the equation above are plotted against the experimental values in order to determine the prediction accuracy:

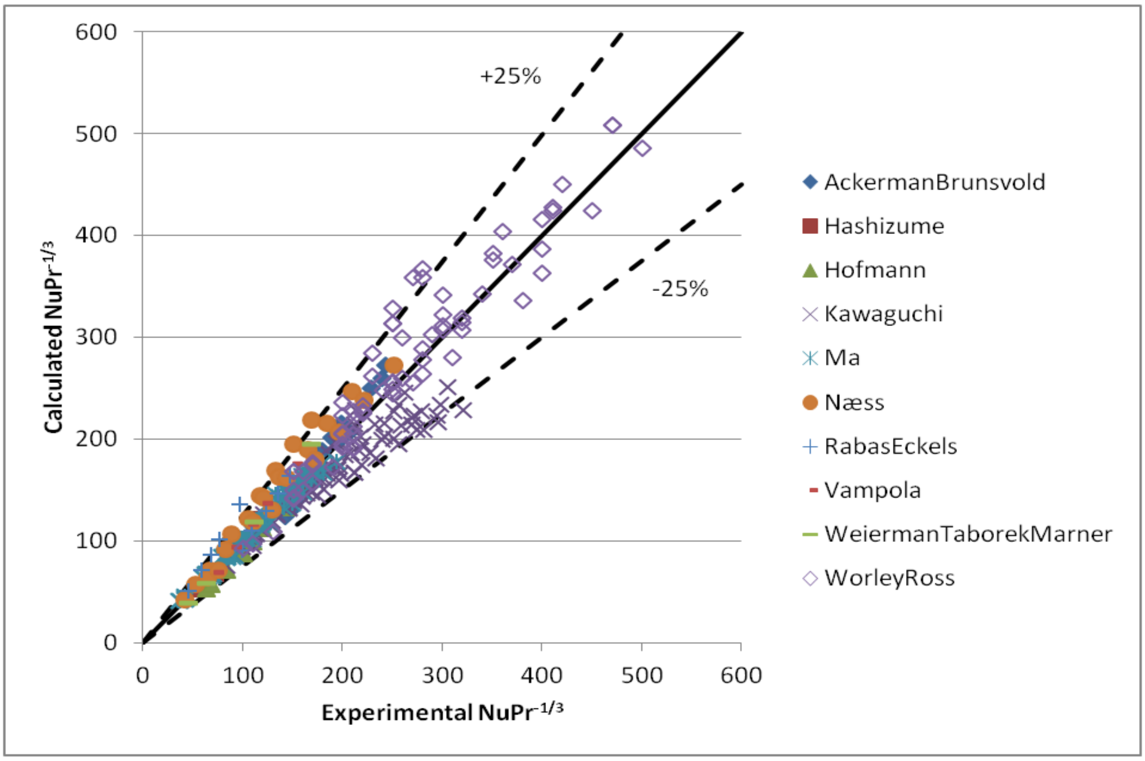

Figure 5 Prediction accuracy of regression equation (eq. 25) for heat transfer (serrated fins)

The figure below shows the calculated value divided by the experimental value plotted against the Reynolds number:

Figure 6 Ratio between calculated (eq. 25) and experimental value against Re (serrated fins)

The data from Rabas and Eckels (1975) were calculated higher than the experimental values (ratio 1,2-1,4 for geometry 3 and 4). It was also seen that geometry 1 from Næss (2007) was overestimated (ratio 1,2-1,3). One reason for this could be the Reynolds number exponent which is higher in this correlation than in the Næss (2007) correlation (0,74 and 0,65 respectively). In addition it can be seen that the data from Kawaguchi et al. (2006b) have a lower calculated value than experimental value. As mentioned, the Kawaguchi et al. (2006b) correlation had a higher exponent for the Reynolds number than the regression equation so this could be the reason why the data are underestimated.

90,2 % of the data were predicted within ±20 %. 71,8 % of the data were predicted within ±10 %.

Further the regression analysis was performed using Ar instead of all the dimensionless groups for fin geometry for the same data as before except from the data from Kawaguchi et al. (2006b)/Kawaguchi et al. (2005) (segment width not given). As in the earlier regression analysis, it was concluded that the data from Cox (1973) and Schryber (1945) were calculated too low and too high respectively. Therefore it was decided to remove those data also in this case. When the regression analysis was performed again without the mentioned data, the following regression equation was developed:

$$Nu \cdot Pr^{-1/3} = 0{,}0821 \cdot Re^{0{,}7396} \cdot \left(\frac{P_t}{d_e}\right)^{0{,}2902} \cdot Ar^{-0{,}0697} \tag{35}$$

The exponent for Ar is quite low, but significant. The exponent for the Reynolds number is in the same range as for the correlation using the dimensionless groups for fin geometry (equation 25), even though the data from Kawaguchi et al. (2005)/Kawaguchi et al. (2006b) were not included. The calculated values using the regression equation above are plotted against the experimental values in the figure below:

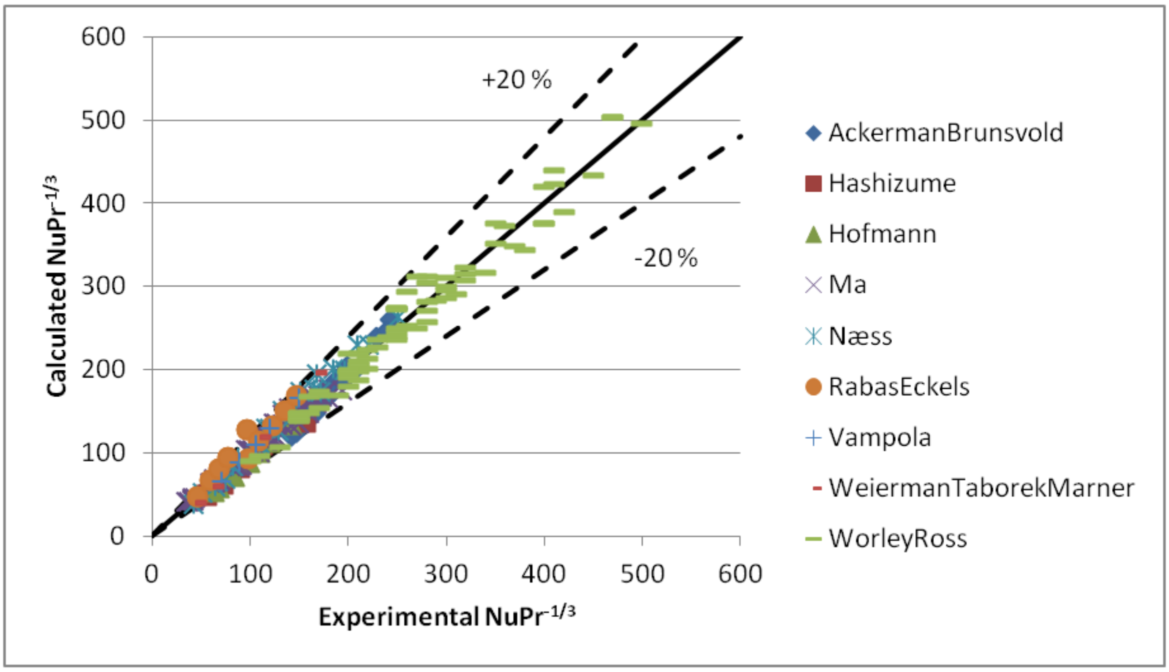

Figure 7 Prediction accuracy of regression equation (eq. 35) for heat transfer (serrated fins, using Ar)

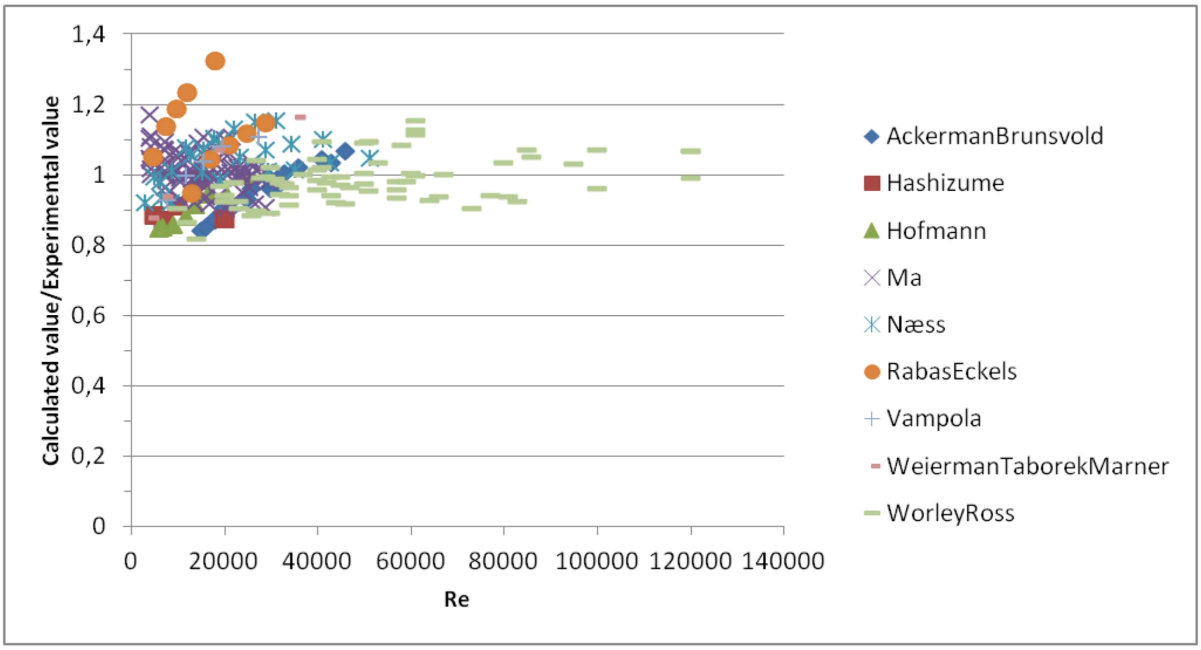

Figure 8 Ratio between calculated (eq. 35) and experimental value against Re (serrated fins)

The regression equation predicted 98,4 % of the data within ±20 % . As can be seen from the figure above, only some data from Rabas and Eckels (1975) were calculated more than 20 %

higher than the experimental values. 81,2 % of the data were predicted within ±10 %. The prediction accuracy is as expected better for this equation, because there are fewer data than in the first case (Kawaguchi et al. (2005)/Kawaguchi et al. (2006b) not included in this case).

The regression analysis of the heat transfer data for $F_t/F_d>1,0$ was performed the following way:

$NuPr^{-1/3}$ was divided by the fin geometry and Reynolds number effect found in for $F_t/F_d<1,0$:

$$C_3 = \frac{Nu \cdot Pr^{-1/3}}{f(fin\ geometry) \cdot Re^m}$$
$$C_3 = \frac{Nu \cdot Pr^{-1/3}}{0,0703 \cdot Re^{0,7404} \cdot \left(\frac{h_e}{s_f}\right)^{-0,20750} \cdot \left(\frac{d_f}{d_e}\right)^{0,5073}} \tag{36}$$

Further the regression was performed using C_3 as the response (i.e. y-variable) and different dimensionless groups for tube bundle layout as predictors.

This led to the following regression equation:

$$Nu \cdot Pr^{-1/3} = 0,1539 \cdot Re^{0,7404} \cdot \left(\frac{h_e}{s_f}\right)^{-0,20572} \cdot \left(\frac{d_f}{d_e}\right)^{0,5073} \cdot \left(\frac{P_t}{P_l}\right)^{-0,7726} \tag{37}$$

The equation shows that increasing the ratio between the transversal and longitudinal tube pitch decreases the heat transfer coefficient for $F_t/F_d>1,0$, which is in agreement with the conclusions from Næss (2007).

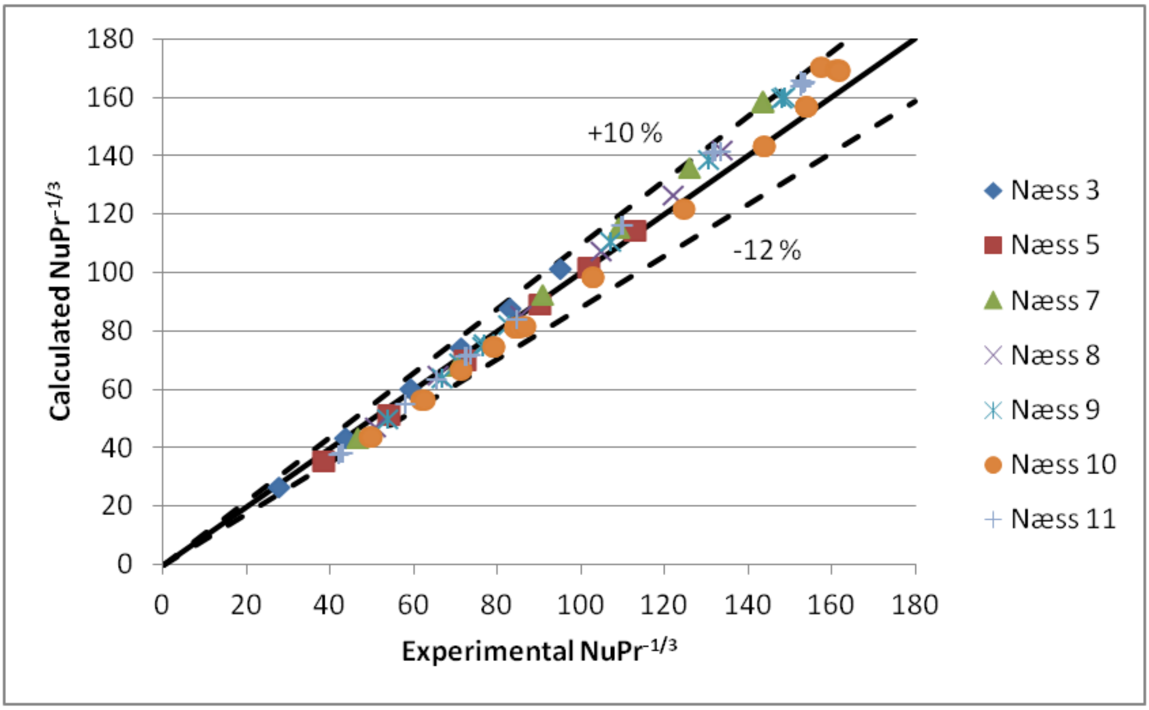

Figure 9 Prediction accuracy for regression equation (eq. 37) for F_t/F_d>1,0 (serrated fins)

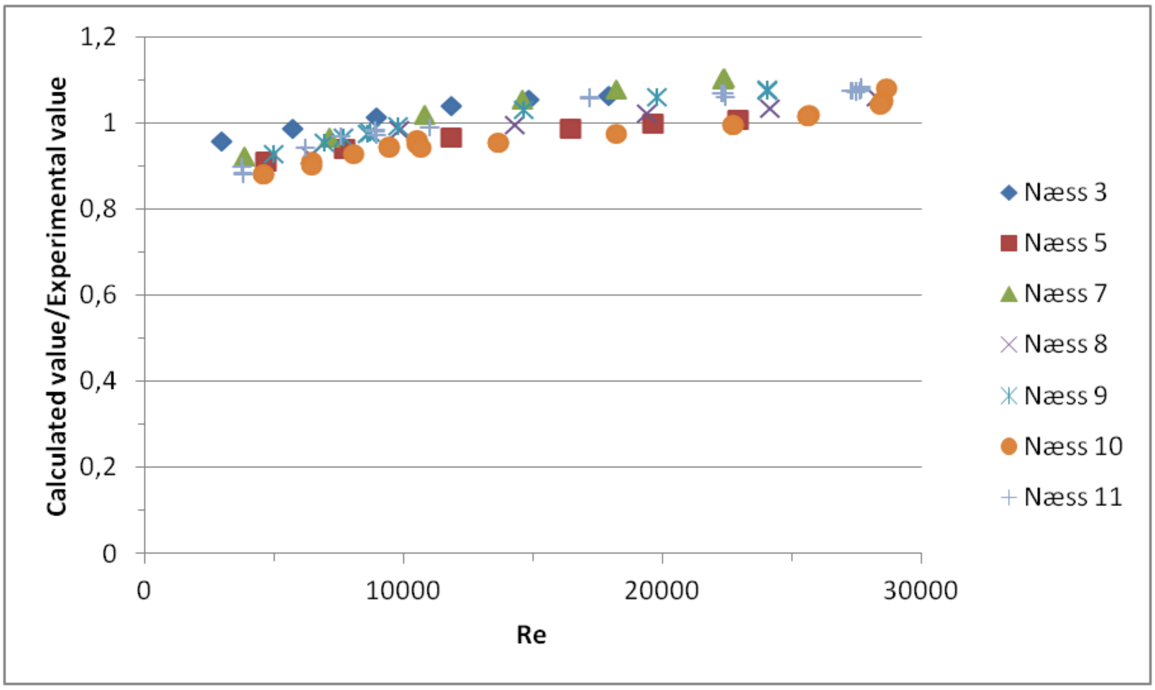

Figure 10 Ratio between calculated (eq. 37) and experimental value vs Re (serrated fins) for F_t/F_d>1,0

All the data were predicted from +10 % to -12 %.

At last the same regression analysis was performed for F_t/F_d>1,0 using the Ar correlation:

$$C_4 = \frac{Nu \cdot Pr^{-1/3}}{f(fin\ geometry) \cdot Re^m} = \frac{Nu \cdot Pr^{-1/3}}{0{,}0821 \cdot Re^{0{,}7396} \cdot Ar^{-0{,}0697}} \quad (38)$$

Regression analysis was performed with C_4 as response and different dimensionless groups for tube bundle layout as predictors. The analysis gave the following regression equation:

$$Nu \cdot Pr^{-1/3} = 0{,}1698 \cdot Re^{0{,}7396} \cdot \left(\frac{P_t}{P_l}\right)^{-0{,}60923} \cdot Ar^{-0{,}0697} \quad (39)$$

Also for this equation the heat transfer coefficient decreases when the ratio between the transversal and longitudinal tube pitch is increased.

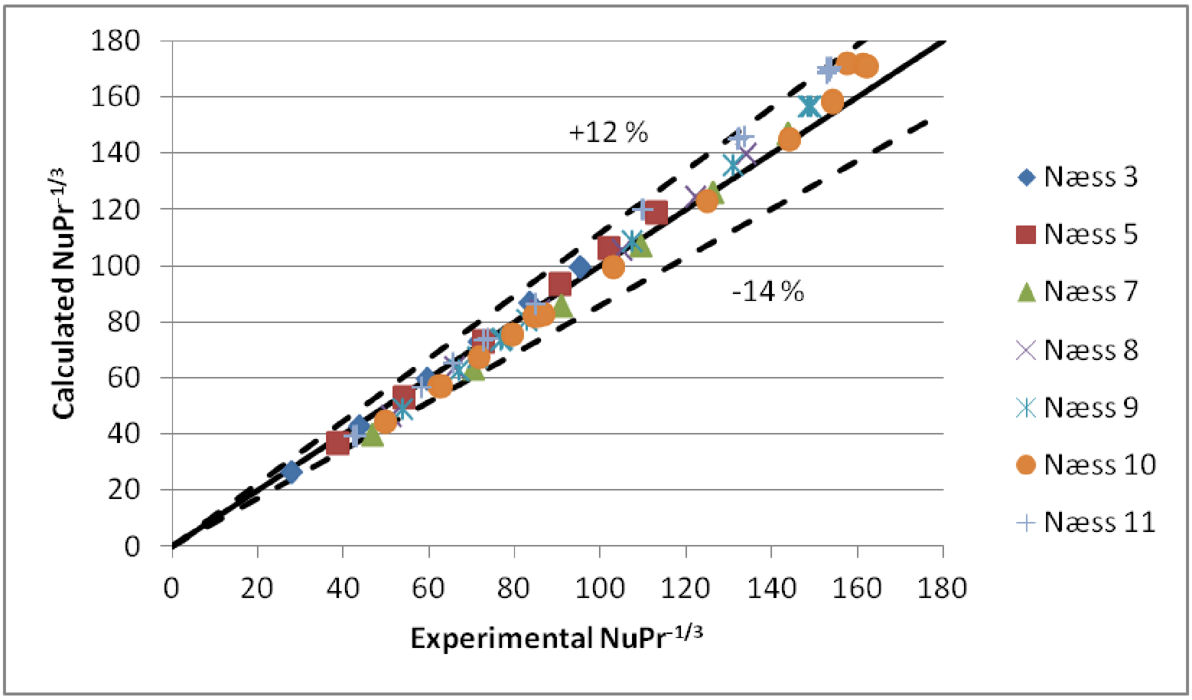

Figure 11 Prediction accuracy for regression equation (eq. 39) using Ar for Ft/Fd>1,0 (serrated fins)

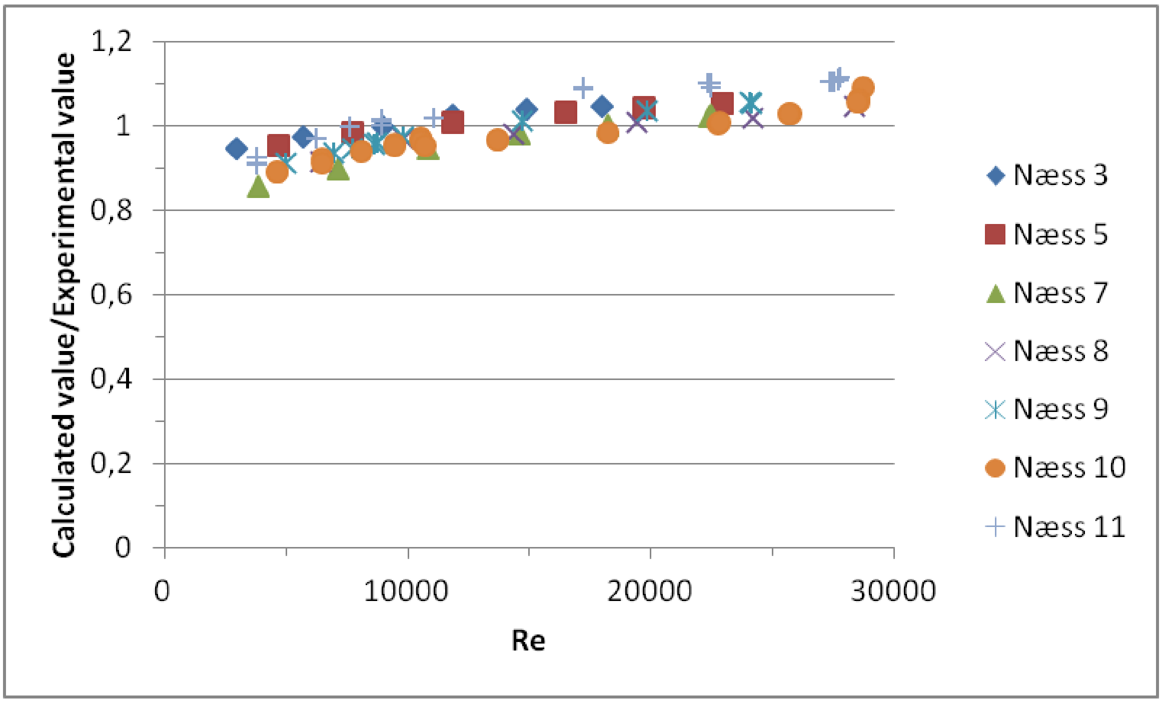

Figure 12 Ratio between calculated (eq. 39) and experimental value vs Re (serrated fins) for $F_t/F_d>1{,}0$

All the data were predicted within +12 % to -14 %.

3.4.2.3 Pressure drop data

Before starting the regression analysis, all the pressure drop data represented as the Euler numbers were plotted against the Reynolds number (Re<50 000) for F_t/F_d<1,0. The Reynolds number restriction (Re<50 000) was chosen because it was observed that the Euler number became approximately constant for Re>50 000:

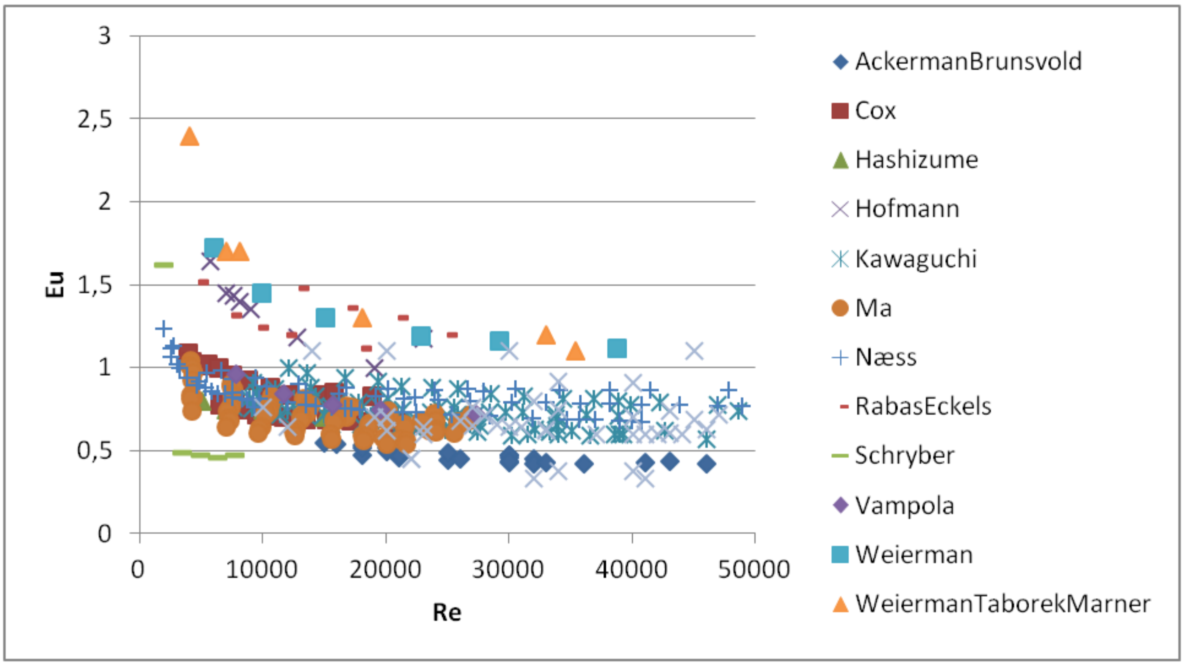

Figure 13 Pressure drop data for serrated fins vs Re

From the inspection of the data it was observed that only for the data from Cox (1973), Hofmann (2009), Kawaguchi et al. (2006a)/ Kawaguchi et al. (2004), Ma et al. (2011), Weierman (1977) and Weierman et al. (1978) there were six or more data points for the Euler number for most of the geometries. Worley and Ross (1960) tested 16 different geometries, but there were only ca. three data points for the Euler number for each geometry.

The following authors had five points for the Euler number for each geometry: Ackerman and Brunsvold (1970), Hashizume (1981), Rabas and Eckels (1975), Schryber (1945) and Vampola (1966).

The regression analysis was first tried for all the data for Re<50 000. This resulted in a model with a very low R^2 (ca. 41 %) and high MSE (Mean square error). A trial and error procedure was performed; here data from the different authors were removed in order to find out if the model was improved. It was observed that the model was improved a lot when the data from the authors with few data points were removed before doing the regression analysis. Therefore only the data from the authors with six or more data points for the Euler number were included in the regression analysis.

The regression analysis using the data from authors with six or more data points resulted in the regression equation below:

$$Eu = 7{,}132 \cdot Re^{-0{,}1775} \cdot \left(\frac{P_t}{d_e}\right)^{-0{,}6928} \cdot \left(\frac{P_l}{d_e}\right)^{-0{,}623} \cdot \left(\frac{h_e}{s_f}\right)^{0{,}2827} \cdot \left(\frac{d_f}{d_e}\right)^{0{,}4954} \tag{40}$$

The regression equation shows that the tube bundle layout has a very large impact on the pressure drop. Both an increase of the transversal and longitudinal tube pitch results in a significant decrease of the Euler number.

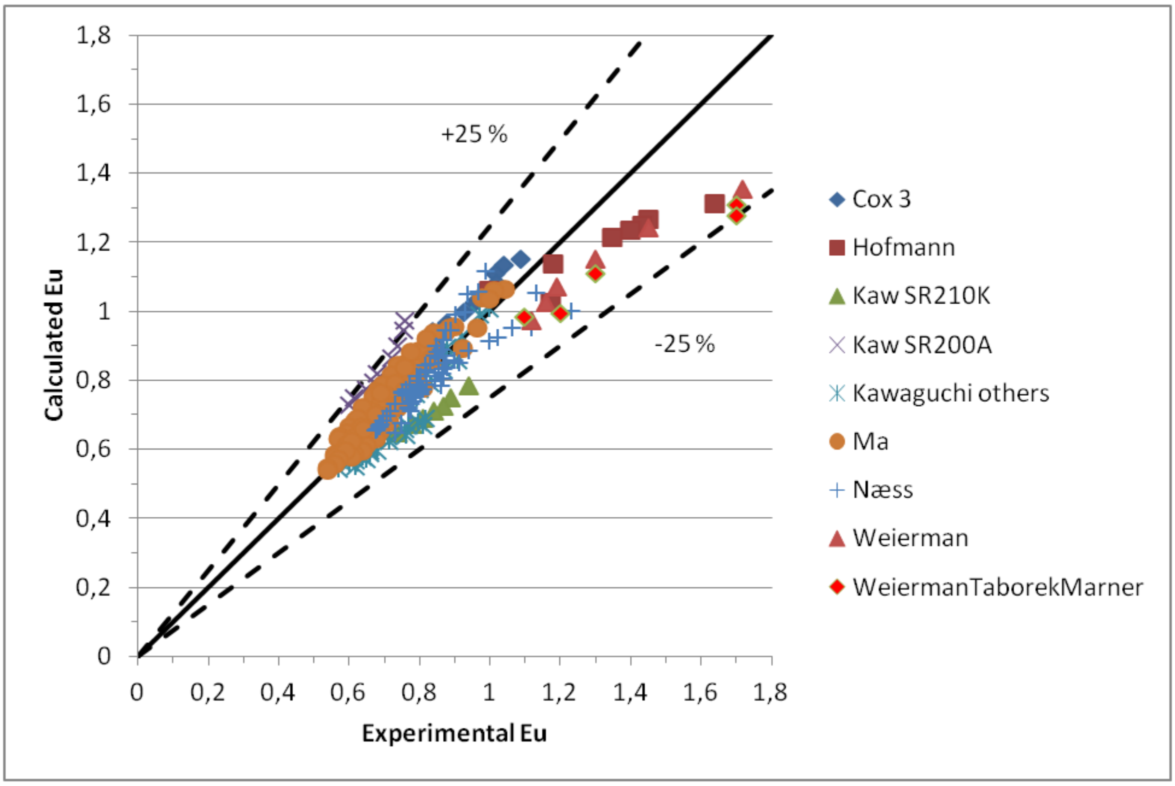

Figure 14 Prediction accuracy of regression equation (eq. 40) for pressure drop (serrated fins),F_t/F_d<1,0

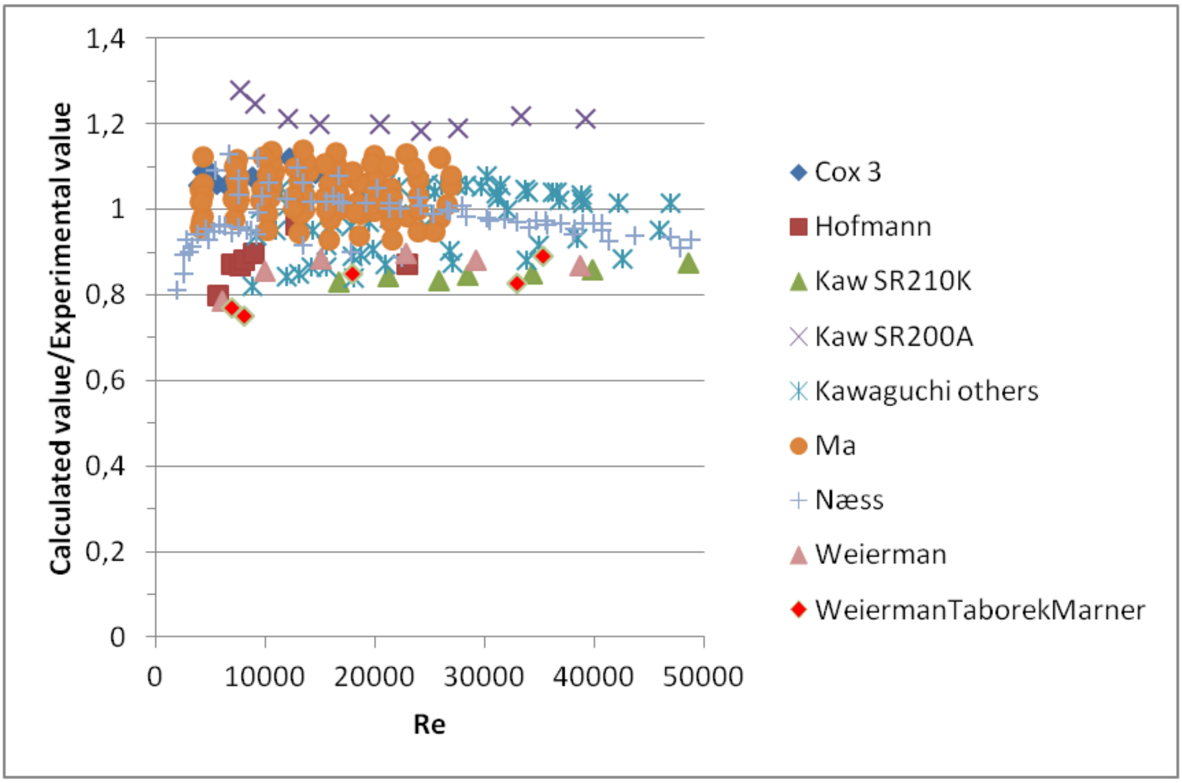

Figure 15 Ratio between calculated value (eq.40) and experimental value vs Re (pressure drop serrated fins) $F_t/F_d<1,0$

The regression equation predicted 96,4 % of the data within ±20 %. 73,8 % of the data were predicted within ±10 %. It is observed that for the high Euler numbers, the equation calculates the Euler numbers lower than they really are (For example Weierman et al. (1978)). In addition the data from geometry SR200A (Kawaguchi et al. (2004)) are calculated ca. 20-30 % higher than the experimental values.

Also for the pressure drop data, a regression equation using Ar instead of all the dimensionless groups for fin geometry was developed. Here the same data were included, except from the data from Kawaguchi et al. (2006a)/Kawaguchi et al. (2004) because Ar could not be calculated for these data (the segment width was not given in the papers).

The regression analysis led to the regression equation below:

$$Eu = 5{,}867 \cdot Re^{-0{,}1804} \cdot \left(\frac{P_t}{d_e}\right)^{-0{,}58387} \cdot \left(\frac{P_l}{d_e}\right)^{-0{,}88026} \cdot Ar^{0{,}4153} \tag{41}$$

As can be seen from the equation, the tube bundle layout is even more important now. This is probably because the data from Kawaguchi et al. (2006a)/Kawaguchi et al. (2004) (where the tube arrangement had no significant effect) were not included.

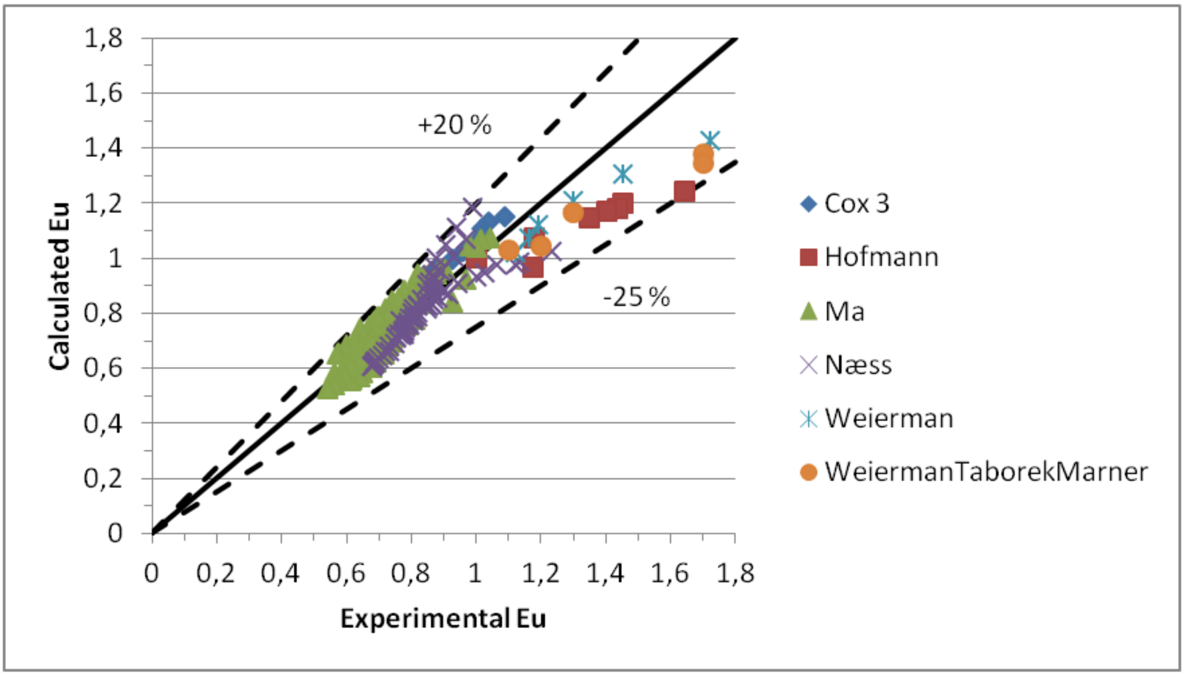

Figure 16 Prediction accuracy of regression equation (eq. 41) using Ar for pressure drop (serrated fins)

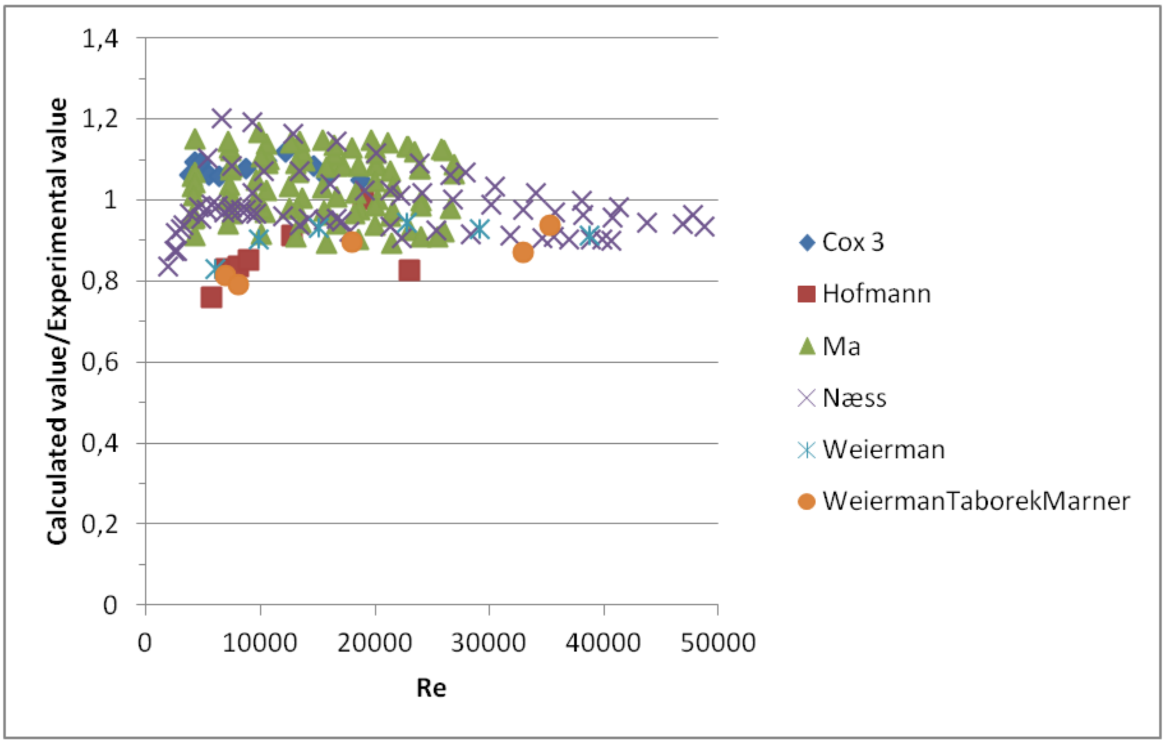

Figure 17 Ratio between calculated value (eq. 41) and experimental value vs Re (serrated fins, pressure drop)

98,5 % of the data were predicted within ±20 %, while 75,9 % of the data were predicted within ±10 %. Also for this regression equation it is seen that for the data with high Euler numbers, the Euler number is calculated lower than the experimental value (for example Hofmann (2009) and Weierman et al. (1978)).

The regression analysis was also tried for $F_t/F_d>1{,}0$ using the same method as for the heat transfer data for serrated fins:

The Euler number was divided by the fin geometry and Reynolds number effect from the correlation for $F_t/F_d<1{,}0$:

$$C_1 = \frac{Eu}{f(fin\ geometry) \cdot Re^m}$$
$$C_1 = \frac{Eu}{7{,}132 \cdot Re^{-0{,}1775} \cdot \left(\frac{h_e}{s_f}\right)^{0{,}2827} \cdot \left(\frac{d_f}{d_e}\right)^{0{,}4954}} \quad (42)$$

The regression analysis was performed with the C_1-values as the response and the dimensionless groups for tube bundle layout as the predictors. This gave the following equation:

$$Eu = 74{,}945 \cdot Re^{-0{,}1775} \cdot \left(\frac{P_t}{d_e}\right)^{-3{,}0779} \cdot \left(\frac{P_l}{d_e}\right)^{0{,}9676} \cdot \left(\frac{h_e}{s_f}\right)^{0{,}2827} \cdot \left(\frac{d_f}{d_e}\right)^{0{,}4954} \quad (43)$$

However, it is not recommended to use this regression equation. The exponent for the ratio between the transversal tube pitch and the effective tube outside diameter is not at all realistic (expected to be in the range 0 to -1). It seems like the method used for the heat transfer data for F_t/F_d>1,0 fails for the corresponding pressure drop data. When using the Ar correlation, the same was observed.

3.4.3 Solid fins

3.4.3.1 The data

The heat transfer data and pressure drop data for solid fins were collected during the project thesis in the autumn 2012 (Feten (2012)). A completely new database was implemented in the database program Filemaker Pro. The database corresponds to the database implemented by Kaspersen (1995) for serrated fins.

Table 2 Data sources for heat transfer and pressure drop for solid fins

	Data	**Fin type**
Ward and Young (1959)	Nu, Eu	I-foot
Briggs and Young (1963)	Nu, Eu	I-foot
Brauer (1964)	Nu, Eu	I-foot
Robinson and Briggs (1966)	Eu	I-foot
Weierman (1977)	Eu	I-foot
Stasiulevicius et al. (1988)	Nu, Eu	I-foot
Kawaguchi et al. (2004)/Kawaguchi et al. (2005)/Kawaguchi et al. (2006a)/Kawaguchi et al. (2006b)	Nu, Eu	I-foot

3.4.3.2 The heat transfer data

In the case of solid fins, all the heat transfer data were for $F_t/F_d<1,0$. The amount of data for heat transfer was less for solid fins than for serrated fins.

Before the regression analysis was started, an inspection of the data was done. This inspection gave the impression that some of the data from Brauer (1964) had rather high values for $NuPr^{-1/3}$ compared to the others. This can be seen in the figure below where the $NuPr^{-1/3}$-values are plotted against the Reynolds number:

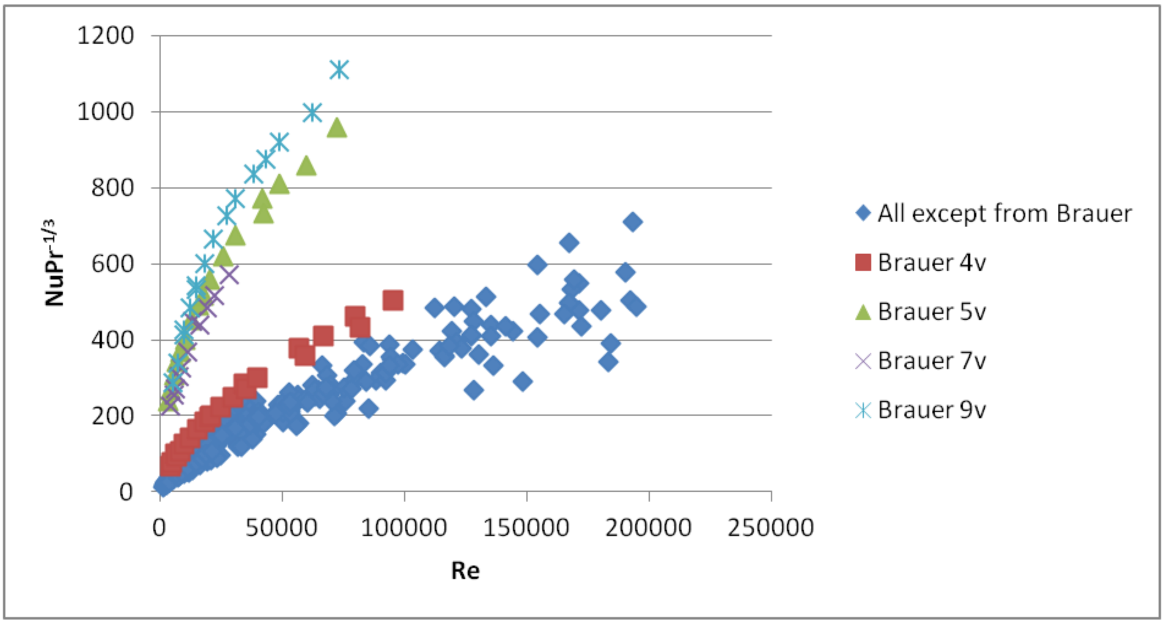

Figure 18 $NuPr^{-1/3}$ against Re for solid fins

Especially the geometries 5v, 7v and 9v from Brauer (1964) did not follow the rest of the data. It was decided to remove these data, because it was seen that the prediction accuracy of the regression equation would increase a lot when removing them.

Also it was observed that there was a quite large amount of data for high Reynolds numbers. This was especially the case for the data from Stasiulevicius et al. (1988). The data from Stasiulevicius et al. (1988) for the high Reynolds numbers were in the turbulent region. Therefore only the heat transfer data for Reynolds numbers less than 50 000 were included in the regression analysis.

The regression analysis using all the data (Except from the mentioned geometries from Brauer (1964)) for Re<50 000 gave the following equation:

$$Nu \cdot Pr^{-1/3} = 0{,}072 \cdot Re^{0{,}7504} \cdot \left(\frac{P_t}{P_l}\right)^{-0{,}22417} \cdot \left(\frac{h_f}{s_f}\right)^{-0{,}34171} \cdot \left(\frac{d_f}{d_e}\right)^{0{,}69323} \cdot \left(\frac{t}{s_f}\right)^{0{,}0732} \quad (44)$$

However, it is not recommended to use this equation as it gives the false impression that the heat transfer coefficient decreases when P_t/P_l is increased. In the correlation from Stasiulevicius et al. (1988) the heat transfer coefficient increases when P_t/P_l is increased. Kawaguchi et al. (2006b) concluded that the tube layout had no impact on the heat transfer. Briggs and Young (1963) and Ward and Young (1959) used the same P_t/P_l for all their geometries. Therefore it is difficult to say why the exponent was negative, but somehow the combination of these data gave a negative exponent.

A trial and error procedure was carried out. Here different data were removed before doing the analysis to see if the exponent changed sign. For some reason the sign of the exponent changed when the data from Kawaguchi et al. (2005)/Kawaguchi et al. (2006b) and geometry 4v from Brauer (1964) were removed. The same happened when the data from Stasiulevicius et al. (1988) and geometry 4v from Brauer (1964) were removed. It seemed like the combination of the data from Kawaguchi et al. (2005)/Kawaguchi et al. (2006b) and Stasiulevicius et al. (1988) gave the negative exponent.

The following regression equation is recommended to use (Kawaguchi et al. (2005)/Kawaguchi et al. (2006b) and geometry 4v from Brauer (1964) were not included in the analysis):

$$Nu \cdot Pr^{-1/3} = 0{,}117 \cdot Re^{0{,}659} \cdot \left(\frac{P_t}{P_l}\right)^{0{,}24502} \cdot \left(\frac{h_f}{s_f}\right)^{-0{,}21808} \cdot \left(\frac{d_f}{d_e}\right)^{0{,}29684} \cdot \left(\frac{s_f}{t}\right)^{0{,}11758} \quad (45)$$

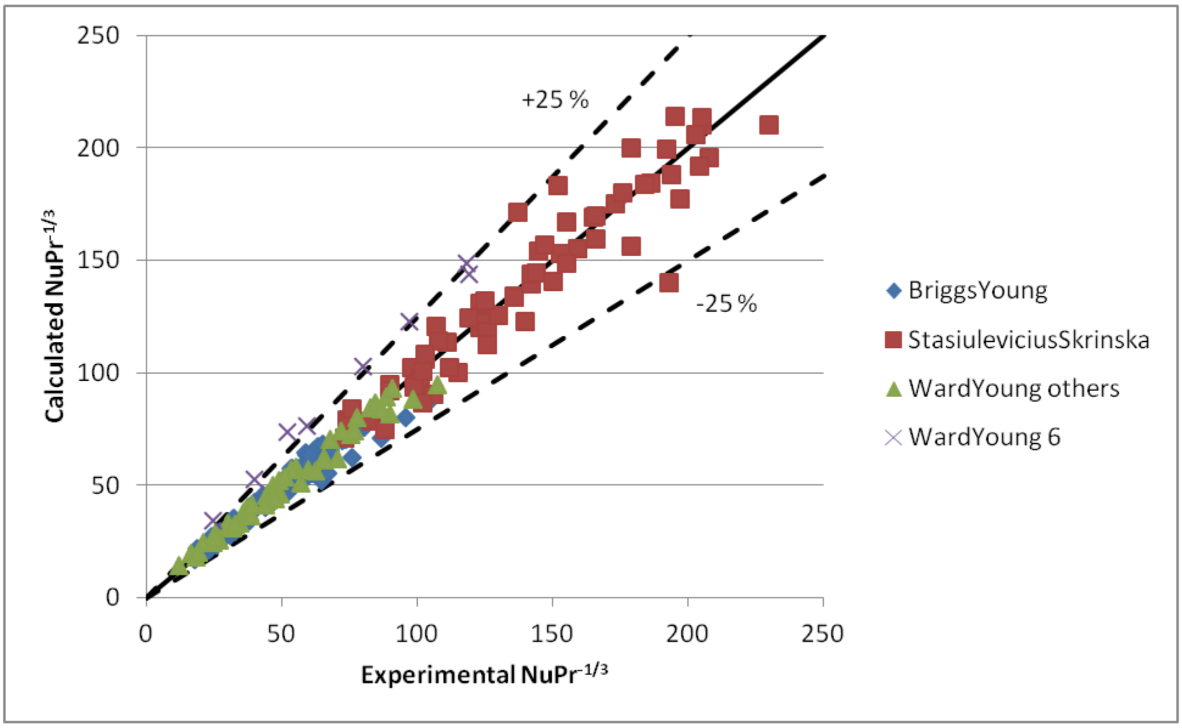

Figure 19 Prediction accuracy of regression equation (eq. 45) for heat transfer (solid fins)

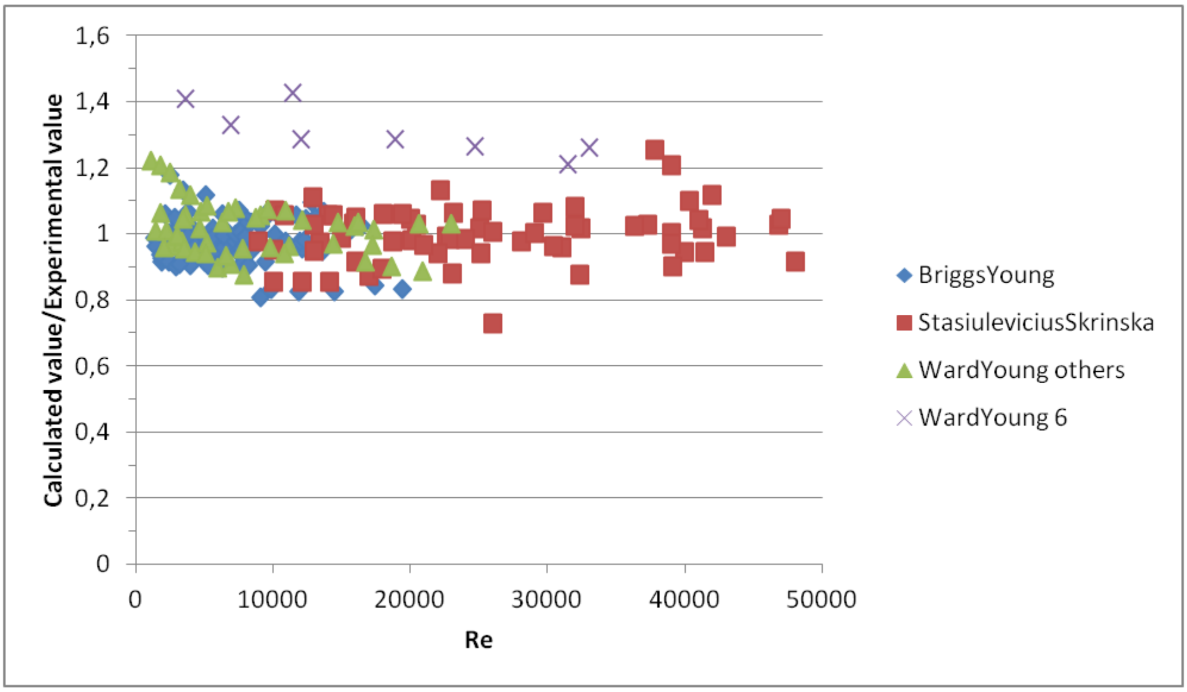

Figure 20 Ratio between calculated (eq. 45) and experimental value vs Re for heat transfer (solid fins)

93,9 % of the data were predicted within ±20 %. Apart from the data for geometry 6 from Ward and Young (1959), almost all the data were predicted within ±20 %. 80,8 % of the data were predicted within ±10 %.

Further Ar was tried as dimensionless group for the same data as above. This resulted in the regression equation below:

$$Nu \cdot Pr^{-1/3} = 0{,}176 \cdot Re^{0{,}652} \cdot \left(\frac{P_t}{P_l}\right)^{0{,}3667} \cdot Ar^{-0{,}0969} \qquad (46)$$

The Reynolds number exponent decreased (as expected) quite a lot when the data from Kawaguchi et al. (2005)/Kawaguchi et al. (2006b) were removed (From 0,75 to ca. 0,65).

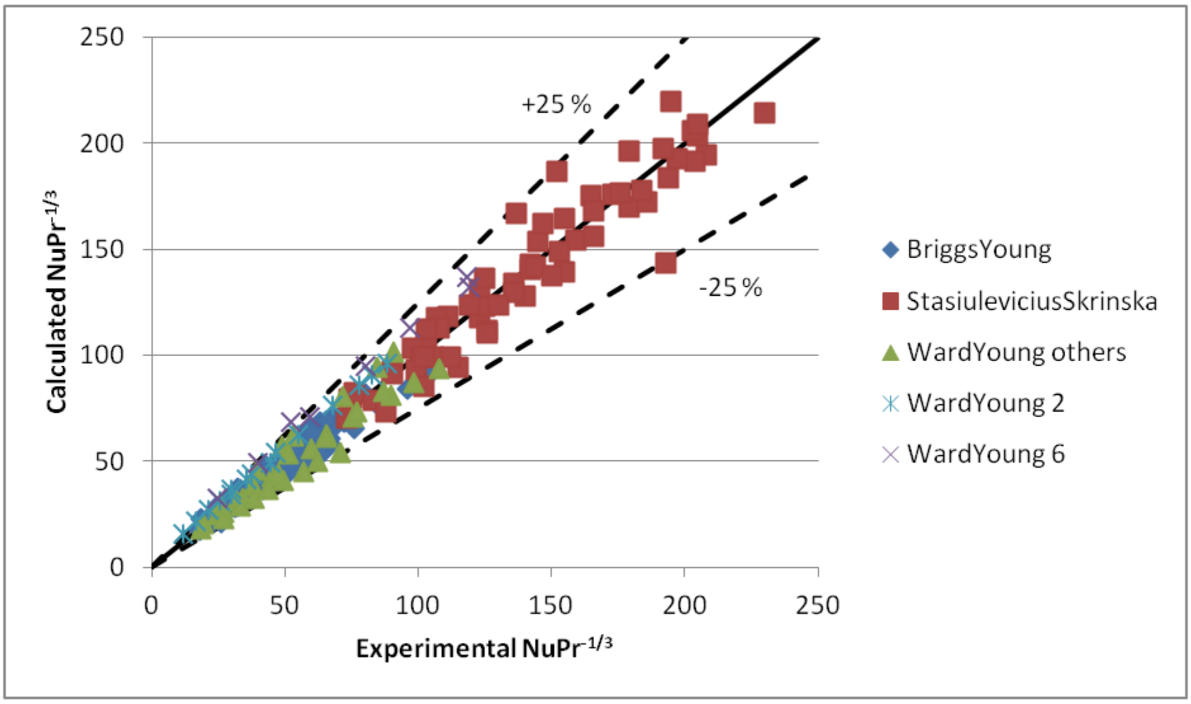

Figure 21 Prediction accuracy of regression equation (eq. 46) using Ar for heat transfer (solid fins)

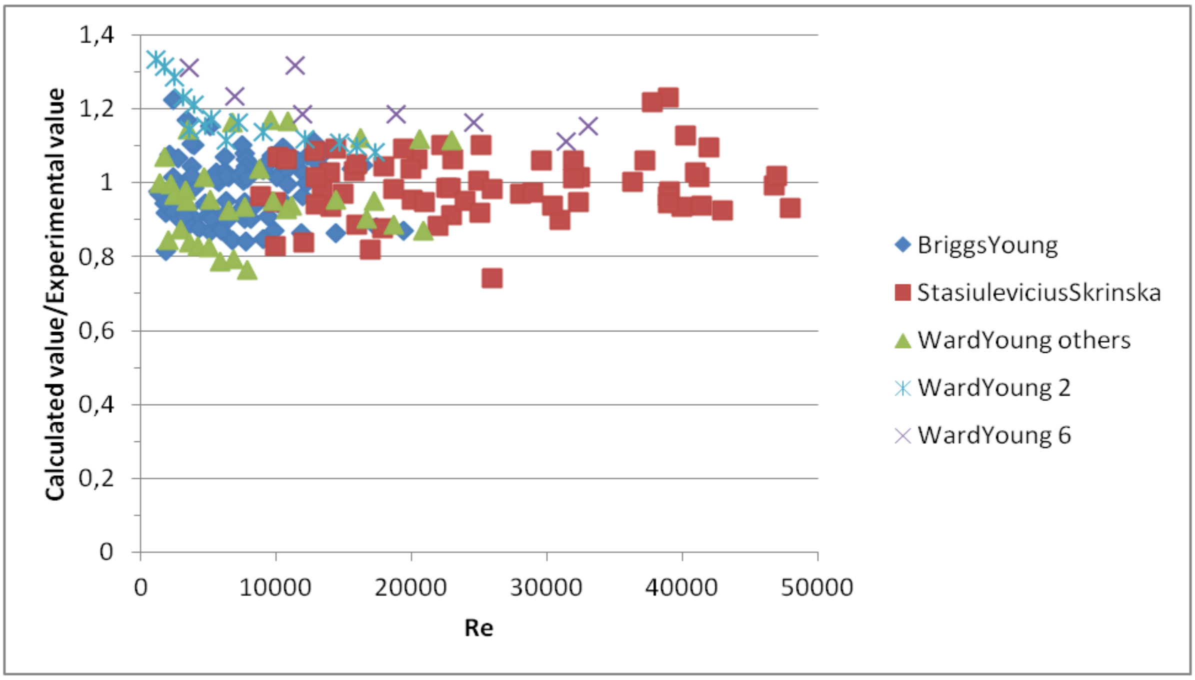

Figure 22 Ratio between calculated (eq. 46) and experimental value for heat transfer (solid fins)

93 % of the data were predicted within ±20 %. Geometries 2 and 6 from Ward and Young (1959) were calculated more than 20 % higher than the experimental values. 65,7 % of the data were predicted within ±10 %. In other words the first version of the regression equation is more accurate (predicted 80,8 % of the data within ±10 %) than the version with Ar.

3.4.3.3 Pressure drop data

First all the pressure drop data (represented as the Euler number) were plotted against the Reynolds number for Re<50 000:

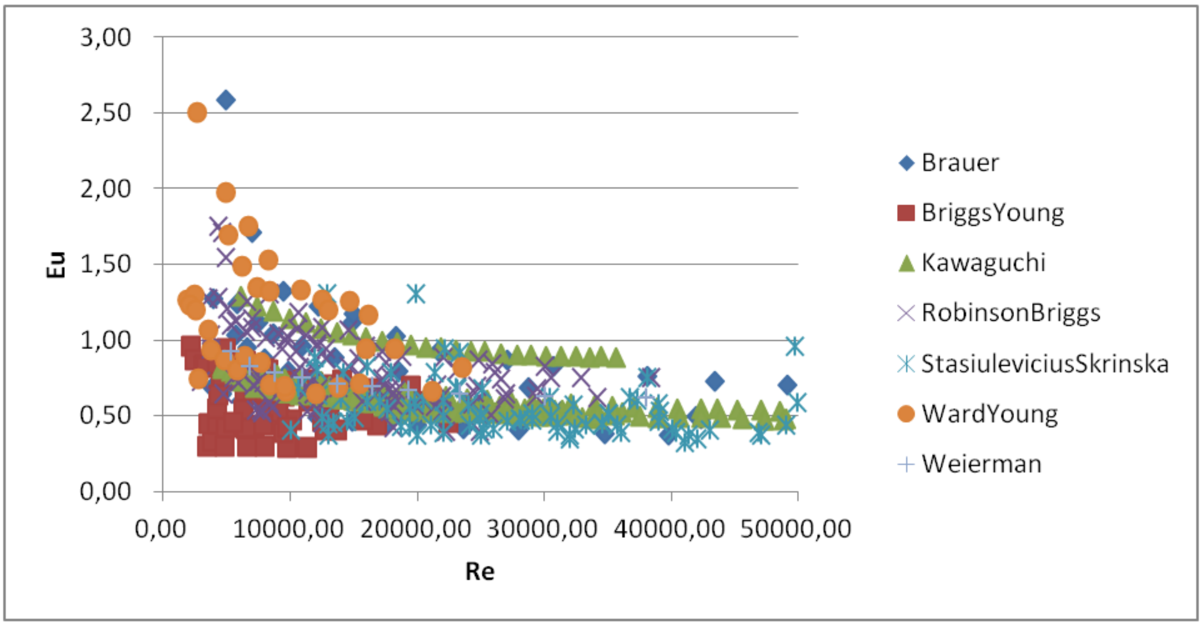

Figure 23 Euler number plotted vs Re for solid fins

The plot showed that some of the geometries from Ward and Young (1959) and one of the geometries from Brauer (1964) had high values for the Euler number compared to the other data. On the other hand, the data from Briggs and Young (1963) had low values for the Euler number compared to the other data.

First the regression analysis was performed using all the data for Re<50 000. The results were quite good, but as expected the geometries mentioned above were underestimated by the equation. In general it looked like the correlation failed for Euler numbers larger than ca. 1,2. The geometries from Briggs and Young (1963) were overestimated.

In order to get a more accurate equation for the rest of the data, all the data from Briggs and Young (1963) and geometry 5v from Brauer (1964) were removed. Also it was decided to perform the analysis for Eu≤1,2. The reason for this choice was the fact that the high Euler numbers were calculated much lower than the experimental values and the prediction accuracy increased for the rest of the data when this restriction was applied. Some of the geometries from Ward and Young (1959) and Stasiulevicius et al. (1988) were removed, because there was a lack of data points (as a consequence of the Euler number restriction).

The regression analysis gave the following regression equation:

$$Eu = 9{,}82 \cdot Re^{-0{,}20979} \cdot \left(\frac{P_t}{d_e}\right)^{-0{,}72394} \cdot \left(\frac{P_l}{d_e}\right)^{-0{,}19613} \cdot \left(\frac{h_f}{s_f}\right)^{0{,}2634} \cdot \left(\frac{t}{s_f}\right)^{0{,}19259} \cdot \left(\frac{d_f}{d_e}\right)^{0{,}3971} \tag{47}$$

The equation is rather complicated and as for serrated fins the tube bundle layout has a mayor effect on the Euler number. Especially the ratio between the transversal tube pitch and the effective tube outside diameter has a large impact on the Euler number in the equation. However, it is observed that P_l/d_e had a larger impact on the pressure drop for serrated fins than for solid fins.

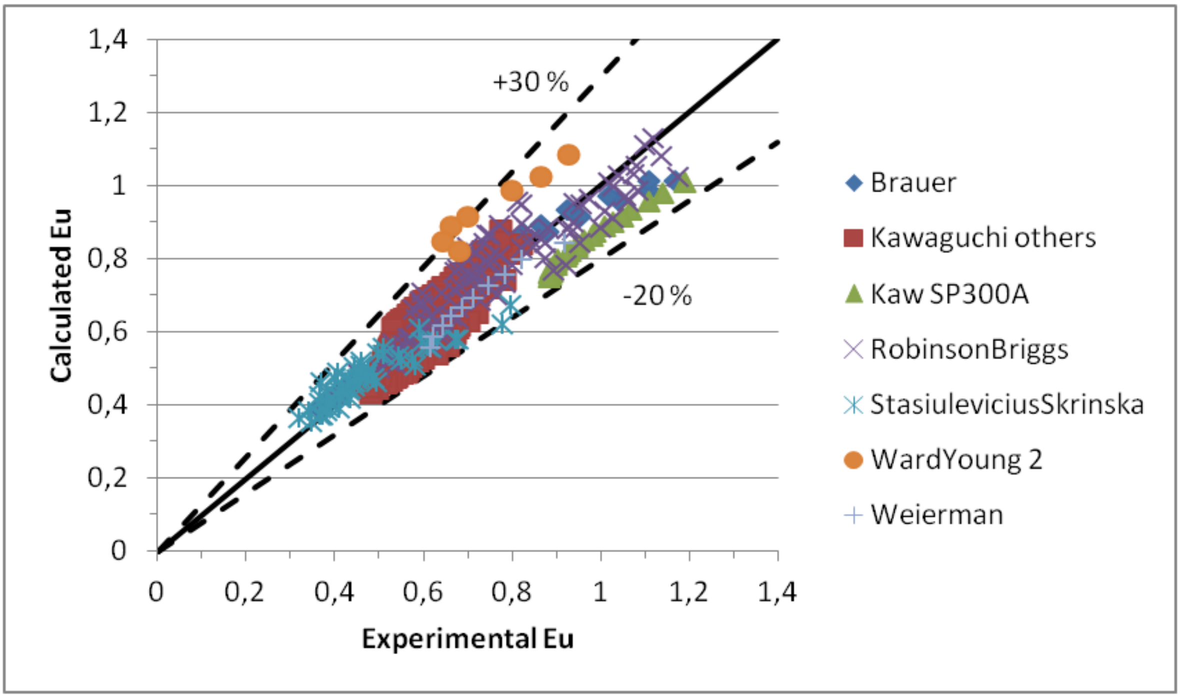

Figure 24 Prediction accuracy of the regression equation (eq. 47) for pressure drop (solid fins)

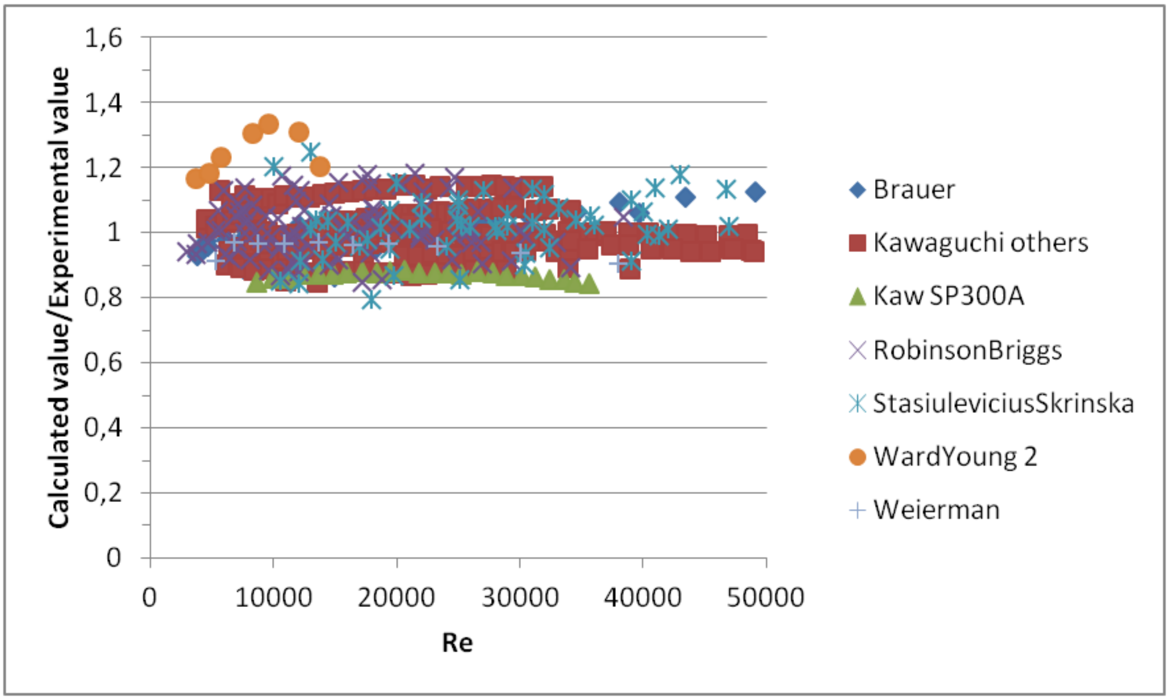

Figure 25 Ratio between calculated (eq. 47) and experimental value vs Re (solid fins, pressure drop)

98 % of the data were predicted within ±20 %, while 70,8 % of the data were predicted within ±10 %. Geometry 2 from Ward and Young (1959) is calculated ca. 20-30 % higher than the experimental values, while the geometry SP300A from Kawaguchi et al. (2004) is calculated ca. 15-18 % lower than the experimental values.

Using Ar as dimensionless group for fin geometry for the same data as above led to the following regression equation:

$$Eu = 4{,}817 \cdot Re^{-0{,}1976} \cdot \left(\frac{P_t}{d_e}\right)^{-0{,}626} \cdot \left(\frac{P_l}{d_e}\right)^{-0{,}28395} \cdot Ar^{0{,}34595} \qquad (48)$$

The transversal tube pitch plays a major role, as it did in the first correlation. In addition, Ar is a significant variable for the Euler number.

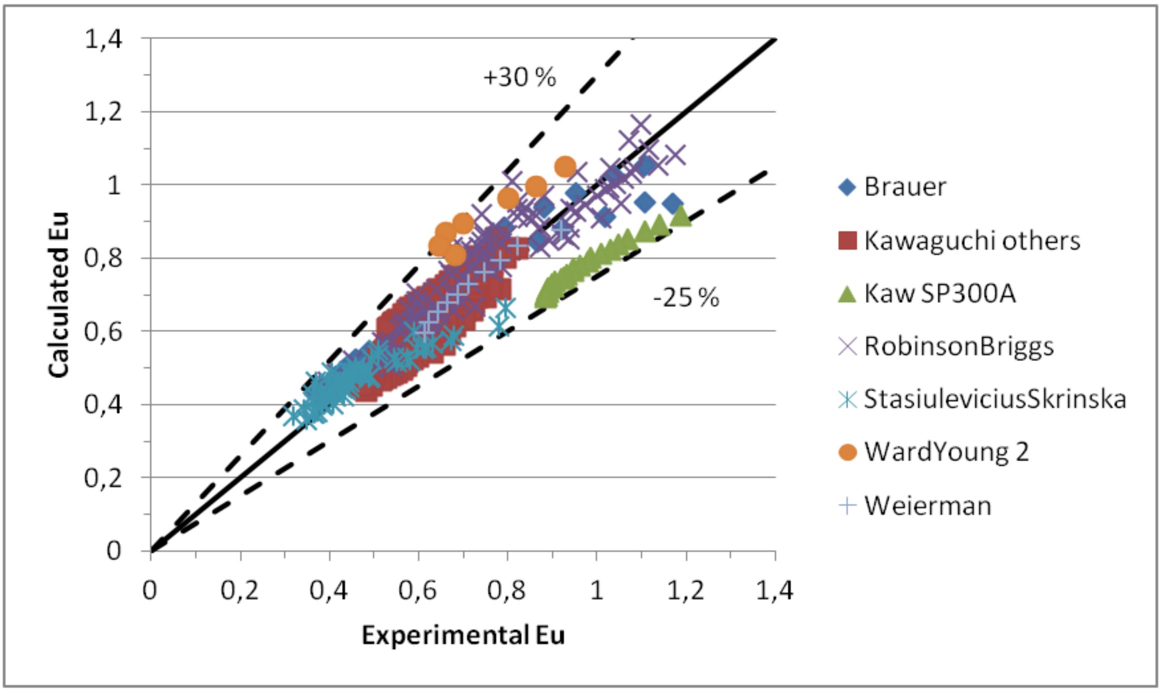

Figure 26 Prediction accuracy of regression equation (eq. 48) for pressure drop (solid fins)

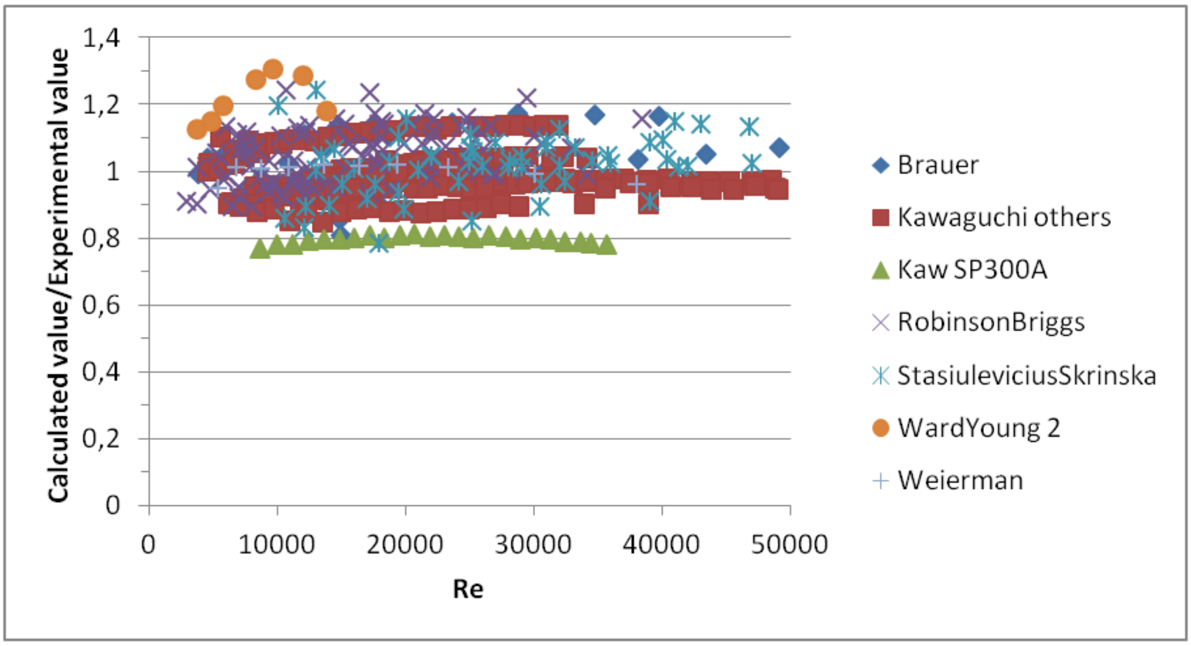

Figure 27 Ratio between calculated (eq. 48) and experimental value vs Re (solid fins, pressure drop)

95,3 % of the data were predicted within ±20 %, while 68,4 % of the data were predicted within ±10 %. In other words the prediction accuracy was a little lower than in the first correlation. Geometry SP300A from Kawaguchi et al. (2004) was calculated ca. 20 % lower than the experimental values, while geometry 2 from Ward and Young (1959) was calculated 15-30 % higher than the experimental values.

3.5 Comparison of correlations

In this section the correlations developed in the regression analysis are compared with the available correlations from the literature (see appendix A for the correlations). The comparison is done for the data used in the regression analysis. The correlations are compared through the ratio between the calculated value and the experimental value for the same Re.

For example: $\frac{Nu \cdot Pr^{-1/3}(Ma\ correlation)}{Nu \cdot Pr^{-1/3}(Experimental)}$

For serrated fins, data for both areas $F_t/F_d<1{,}0$ and $F_t/F_d>1{,}0$ are available. For this comparison only the data for $F_t/F_d<1{,}0$ were used, because the correlations are developed for the data where F_t/F_d is less than one.

3.5.1 Heat transfer correlations for serrated fins

In the table below the percents of the data predicted within the given intervals are presented (using equation 25, presented in chapter 3.4.2.2). 337 data points were used:

Table 3 Prediction accuracy for the heat transfer correlations (serrated fins) $F_t/F_d<1{,}0$

$\frac{Nu \cdot Pr^{-1/3}(calc.)}{Nu \cdot Pr^{-1/3}(exp.)}$	±30 %	±20 %	±10 %
Weierman	99,40 %	86,10 %	52,50 %
Worley/Ross	92,60 %	78 %	41,50 %
Biraghi	88,70 %	77,20 %	42,80 %
Ackerman/Brunsvold	83,90 %	67,70 %	39,50 %
ESCOA	96,40 %	81 %	45,10 %
Hofmann	89,60 %	77,20 %	43,60 %
Ma	97,60 %	89,60 %	59,90 %
Næss	88,10 %	67,40 %	37,10 %
New correlation (Equation 25)	97,60 %	90,20 %	71,80 %

It can be seen from the table above that the correlation from the regression analysis predicts the data better than the other correlations. However, for the prediction intervals ±30 % and ±20 %, the correlation is only slightly better than the correlation from Ma et al. (2011). For the prediction interval ±10 %, the correlation from the regression analysis is clearly better than the others. The correlation from Weierman (McKetta (1992)) predicts almost all the data within ±30 %.

Also, the Ar correlation (equation 35) was compared to the other correlations. As mentioned, the data set was smaller in this case because Ar could not be calculated for the geometries from Kawaguchi et al. (2006b)/Kawaguchi et al. (2005). 251 data points were used:

Table 4 Prediction accuracy for the heat transfer correlations (serrated fins, Ar) $F_t/F_d<1,0$

$\frac{Nu \cdot Pr^{-1/3}(calc.)}{Nu \cdot Pr^{-1/3}(exp.)}$	±30 %	±20 %	±10 %
Weierman	99,60 %	88,80 %	55,40 %
Worley/Ross	100 %	95,20 %	55,80 %
Biraghi	90,80 %	83,70 %	49,40 %
Ackerman/Brunsvold	81,30 %	67,30 %	39,80 %
ESCOA	95,20 %	78,50 %	43,80 %
Hofmann	94,40 %	88,80 %	55 %
Ma	99,20 %	97,60 %	76,10 %
Næss	98 %	84,50 %	49 %
PFR	100 %	95,60 %	68 %
New correlation (Equation 25)	96,80 %	91,60 %	76,50 %
New Ar correlation (equation 35)	99,20 %	98,40 %	81,30 %

Also in this case the regression equation developed in the analysis is slightly better than the correlation from Ma et al. (2011). Also it is observed that the correlations from Worley and Ross (1960) and PFR (1976) manage to predict all the data within ±30 %. The Ar correlation did not manage this, because two data points from Rabas and Eckels (1975) were predicted ca. 32,5 % higher than the experimental values.

3.5.2 Heat transfer correlations for solid fins

The same comparison was done for the heat transfer correlations for solid fins. However, in this case the two correlations were developed for the same amount of data. 213 data points were used:

Table 5 Prediction accuracy for the heat transfer correlations (solid fins)

$\frac{Nu \cdot Pr^{-1/3}(calc.)}{Nu \cdot Pr^{-1/3}(exp.)}$	±30 %	±20 %	±10 %
Briggs/Young	94,80 %	91,50 %	69 %
Stasiulevicius/Skrinska	96,70 %	78,40 %	45,50 %
Ward/Young	84,00 %	60,60 %	35,70 %
PFR	89,20 %	74,60 %	46,50 %
Schmidt	93 %	73,20 %	33,80 %
VDI	92 %	80,80 %	38,50 %
Weierman	33,80 %	8,90 %	3,75 %
New correlation (equation 45)	98,60 %	93,90 %	80,80 %
New correlation Ar (equation 46)	98,10 %	93,00 %	65,70 %

The first heat transfer correlation using the dimensionless groups for fin geometry (equation 45) is the best. It is observed that this correlation predicts a large amount of the data within ±10 % compared to the other correlations. The Ar correlation is almost as good as the first correlation in order to predict the data within ±20 % and ±30 %. The correlation from Briggs and Young (1963) predicts the data better than the other authors, but this was expected as a rather large amount of the data included in the data analysis were from Briggs and Young (1963).

3.5.3 Pressure drop correlations for serrated fins

The same comparison was performed using the available correlations for the Euler number. The table below presents the prediction accuracy of the correlations for the data used to develop the regression equation (equation 40). 275 data points were used:

Table 6 Prediction accuracy for pressure drop correlations for F_t/F_d<1,0 (serrated fins)

$\frac{Eu(calc)}{Eu(exp)}$	±30 %	±20 %	±10 %
Biraghi	90,20 %	83,30 %	50,50 %
Weierman	92,40 %	65,50 %	26,90 %
Næss	60,00 %	53,10 %	42,50 %
Ma	47,30 %	37,10 %	34,90 %
Kawaguchi	65,50 %	63,30 %	45,8 %
New correlation (equation 40)	100 %	96,40 %	73,80 %

The correlation from the regression analysis predicts the data much better than the other correlations. The correlation from Biraghi (Kaspersen (1995)) is the second best. The fact that this correlation is only a function of the Reynolds number could be the reason why it predicts most of the data within ±30 %. The correlations from Næss (2010) and Kawaguchi et al. (2006a) fail to predict the data from Ma et al. (2011) and vice versa. Therefore the prediction accuracy for those three correlations is smaller than for the other correlations.

The Ar correlation (equation 41) was also compared to the other correlations (the data from Kawaguchi et al. (2006a)/Kawaguchi et al. (2004) not included here). The data set contained 195 data points for the Euler number (see table next page):

Table 7 Prediction accuracy for Ar correlation for pressure drop (serrated fins)

$\frac{Eu(calc)}{Eu(exp)}$	±30 %	±20 %	±10 %
Biraghi	86,20 %	76,90 %	49,20 %
Weierman	89,20 %	62,60 %	27,70 %
Næss	48,70 %	48,20 %	34,80 %
Ma	57,90 %	52,30 %	49,20 %
Kawaguchi	48,70 %	48,20 %	34,80 %
New correlation (equation 40)	100 %	98,50 %	77,40 %
Ar correlation (equation 41)	100 %	98,50 %	75,90 %

The Ar correlation is very accurate compared to the other correlations. It is also seen that the first correlation developed (using dimensionless groups for fin geometry) has ca. the same prediction accuracy as the Ar correlation. Also for this amount of data the Biraghi (Kaspersen (1995)) correlation is the best one from the available literature.

3.5.4 Pressure drop correlations for solid fins

The comparison of the new correlations and the correlations from the literature for pressure drop for solid fins gave the results tabulated below:

Table 8 Prediction accuracy of the pressure drop correlations (solid fins)

$\frac{Eu(calc)}{Eu(exp)}$	±30 %	±20 %	±10 %
Weierman	99,30 %	89,20 %	50,20 %
Stasiulevicius/Skrinska	79,0 %	66,40 %	33,80 %
Robinson/Briggs	72,80 %	51,20 %	26 %
Ward/Young	69,60 %	56,10 %	43,10 %
New correlation (equation 47)	99,30 %	98 %	70,80 %
New Ar correlation (equation 48)	99,80 %	95,10 %	68,40 %

The table above shows that the new correlations from the regression analysis are much more accurate than most of the correlations from the literature. The correlation from Weierman (McKetta (1992)) also predicts most of the data within ±20 %. The two correlations from the regression analysis are evenly good. A total of 408 data points were included in the analysis, and therefore it was quite impressive that both of the correlations from the analysis manage to predict almost all of the data within ±20 %.

3.6 Sensitivity analysis

A sensitivity analysis was performed for the heat transfer and pressure drop correlations developed through the regression analysis. The aim was to find how a change in the different variables influenced $NuPr^{-1/3}$ and Eu. It was decided to use a reference geometry (Geometry 1 from Ma et al. (2011) for serrated fins and geometry 27 from Robinson and Briggs (1966) for solid fins) and change every parameter by ±25 %. The analysis was performed for both versions of the correlation (both the one using the dimensionless groups for fin geometry and tube bundle layout, and the one using Ar and the dimensionless groups for tube bundle layout).

The following parameters were changed with ±25 %:

1) Fin height, h_f

2) Tube outside diameter, d_o

3) Fin thickness, t

4) Fin pitch, s_f

5) Segment width, w_f (for serrated fins)

6) Transversal tube pitch, P_t

7) Longitudinal tube pitch P_l

8) ρu (in order to find the effect of the Reynolds number)

Table 9 Reference geometries for the sensitivity analysis

Geometry:	1 from Ma et al. (2011)	27 from Robinson and Briggs (1966)
h_f (mm)	16	14,5
d_o (mm)	38,1	40,9
t (mm)	1	0,46
s_f (mm)	3,89	3,22
w_f (mm)	4	-
P_t (mm)	88	114,05
P_l (mm)	92	98,77

3.6.1 Heat transfer correlations for serrated fins

The results from the sensitivity analysis for the heat transfer correlation using the different dimensionless groups for fin geometry (equation 25) are shown in the figure below. There are two columns for each parameter; the column $NuPr^{-1/3}$ low/$NuPr^{-1/3}$ nom is the ratio between the $NuPr^{-1/3}$-value calculated when the parameter is reduced by 25 % and the $NuPr^{-1/3}$-value for the reference geometry. The other column is the ratio between the calculated value when the parameter is increased by 25 % and the value for the reference geometry.

For example for the parameter h_f:

$$\frac{Nu \cdot Pr^{-1/3}\ low}{Nu \cdot Pr^{-1/3}\ nom} = \frac{Nu \cdot Pr^{-1/3}(h_f\ reduced\ by\ 25\ \%)}{Nu \cdot Pr^{-1/3}\ (reference\ geometry)} \tag{49}$$

$$\frac{Nu \cdot Pr^{-1/3}\ high}{Nu \cdot Pr^{-1/3}\ nom} = \frac{Nu \cdot Pr^{-1/3}(h_f\ increased\ by\ 25\ \%)}{Nu \cdot Pr^{-1/3}(reference\ geometry)} \tag{50}$$

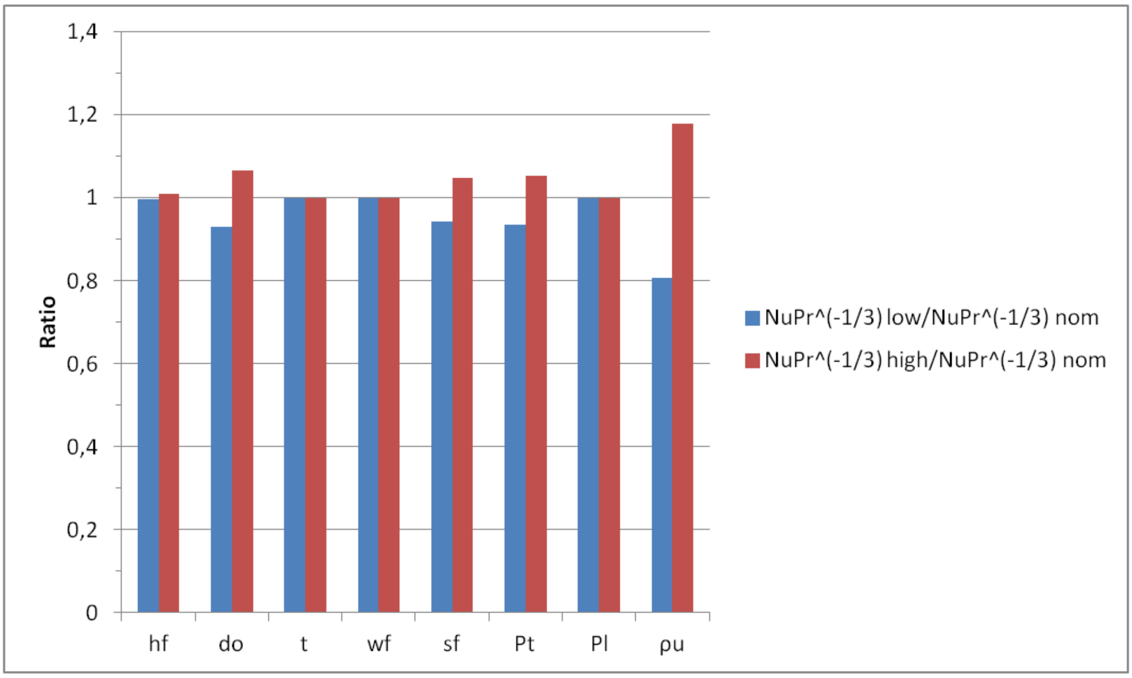

Figure 28 Sensitivity analysis heat transfer correlation for serrated fins (equation 25)

The figure above shows that the Reynolds number was the most significant variable, as expected. The parameters d_o, P_t and s_f had a significant impact on the heat transfer coefficient. An increase in these parameters will increase the heat transfer coefficient. The effect of the fin height seemed to be small. The longitudinal tube pitch, the fin thickness and the segment width had no impact on the heat transfer.

The same analysis for the Ar correlation (equation 35) gave the following results:

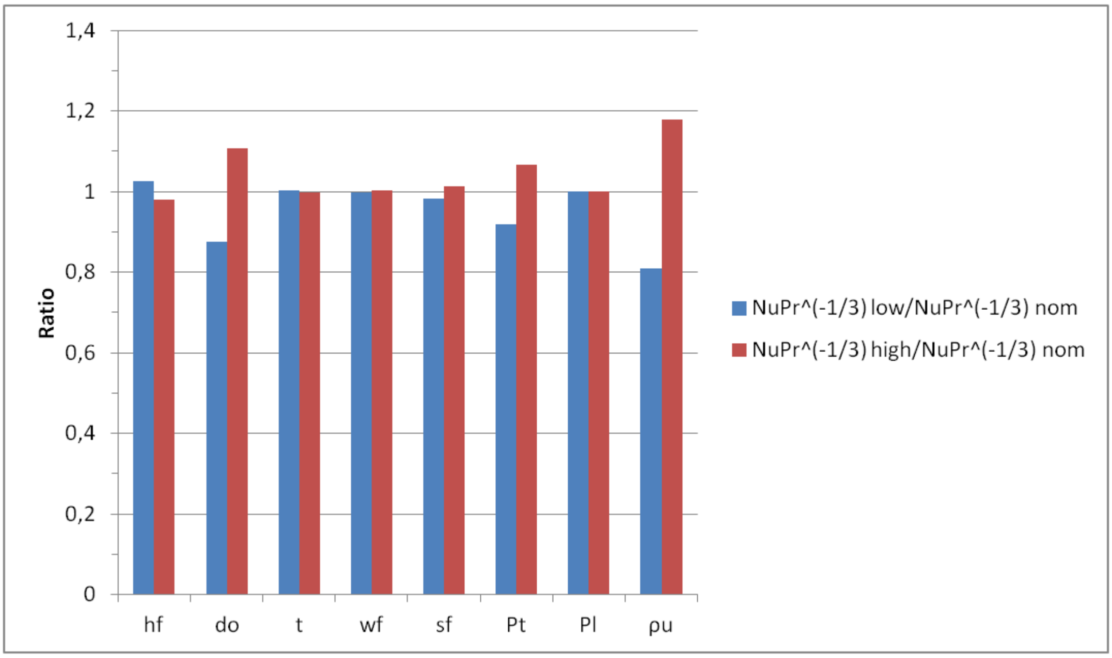

Figure 29 Sensitivity analysis heat transfer correlation (using Ar) for serrated fins (equation 35)

The same things were observed for the Ar correlation. The Reynolds number was the most significant variable. An increase in d_o, P_t and s_f increased the heat transfer coefficient. However, s_f seemed less significant than in the first correlation. Also an increase in h_f decreased the heat transfer coefficient slightly. Though Ar depends on the fin thickness and the segment width, the impact of the two parameters was not significant. The longitudinal tube pitch had no effect on the heat transfer.

3.6.2 Heat transfer correlations for solid fins

The figure below shows the results from the sensitivity analysis for the heat transfer correlation using the dimensionless groups for fin geometry (equation 45):

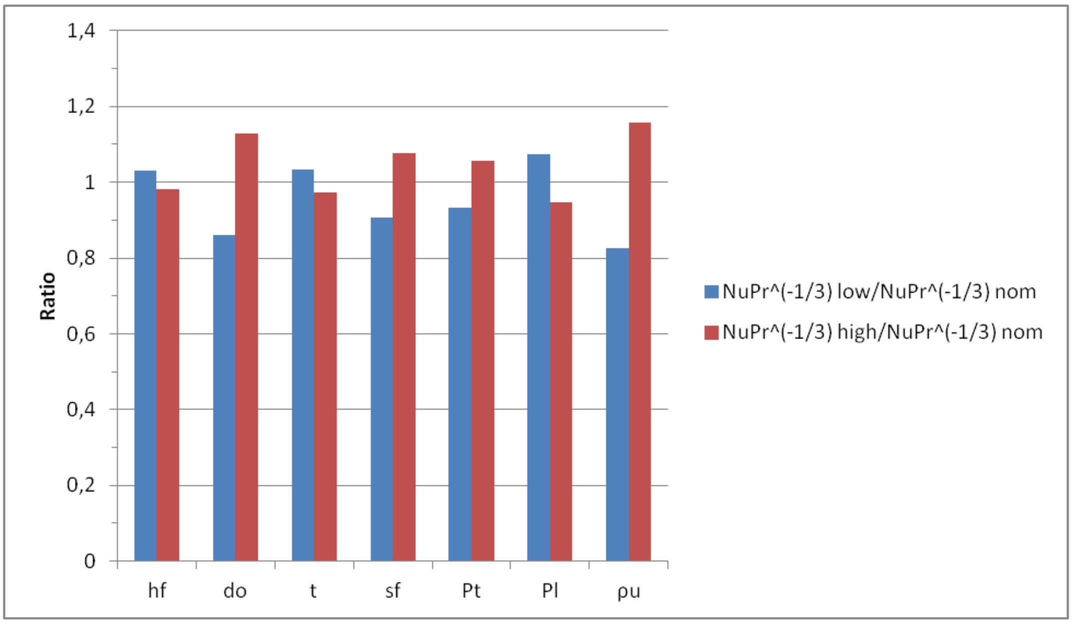

Figure 30 Sensitivity analysis heat transfer correlation for solid fins (equation 45)

The trends were very much the same as for the heat transfer correlations for serrated fins. The Reynolds number was the most significant variable. An increase in d_o, P_t and s_f resulted in a significant increase of the heat transfer coefficient. The flow changes when the tube outside diameter is varied. The velocity at the narrowest cross section is raised to a certain extent with increasing the tube outside diameter and the recirculation zone behind the tube is also increased, Mon (2003). According to Mon (2003), increasing the fin pitch gives a thinner boundary layer which leads to a higher heat transfer coefficient. When the fin height or the fin thickness was increased, the heat transfer coefficient decreased slightly. Contrary to the correlations for serrated fins the longitudinal tube pitch had an impact on the heat transfer coefficient for this correlation. The increase in P_l resulted in a decreasing heat transfer coefficient.

The same analysis for the heat transfer correlation using Ar (equation 46) gave the results in the diagram below:

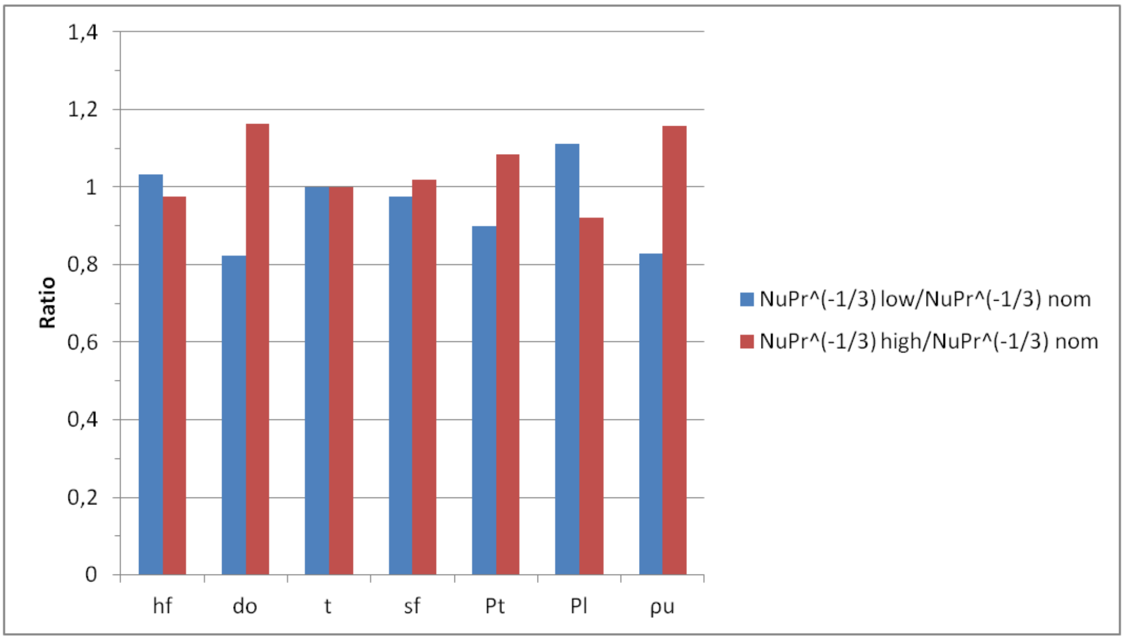

Figure 31 Sensitivity analysis heat transfer correlation (using Ar) for solid fins (equation 46)

The tube bundle layout variables were more important in this correlation than in the first version. On the other hand, the significance of the fin pitch was less in this correlation than in the first version. It was also observed that the tube outside diameter was as important as the Reynolds number.

3.6.3 Pressure drop correlations for serrated fins

The sensitivity analysis of the pressure drop correlations was performed the same way as for the heat transfer correlations. For example for the parameter d_o:

$$\frac{Eu\ low}{Eu\ nom} = \frac{Eu(d_o - 25\ \%)}{Eu(reference\ geometry)} \tag{51}$$

$$\frac{Eu\ high}{Eu\ nom} = \frac{Eu(d_o + 25\ \%)}{Eu(reference\ geometry)} \tag{52}$$

The results from the analysis are shown in the column diagram below:

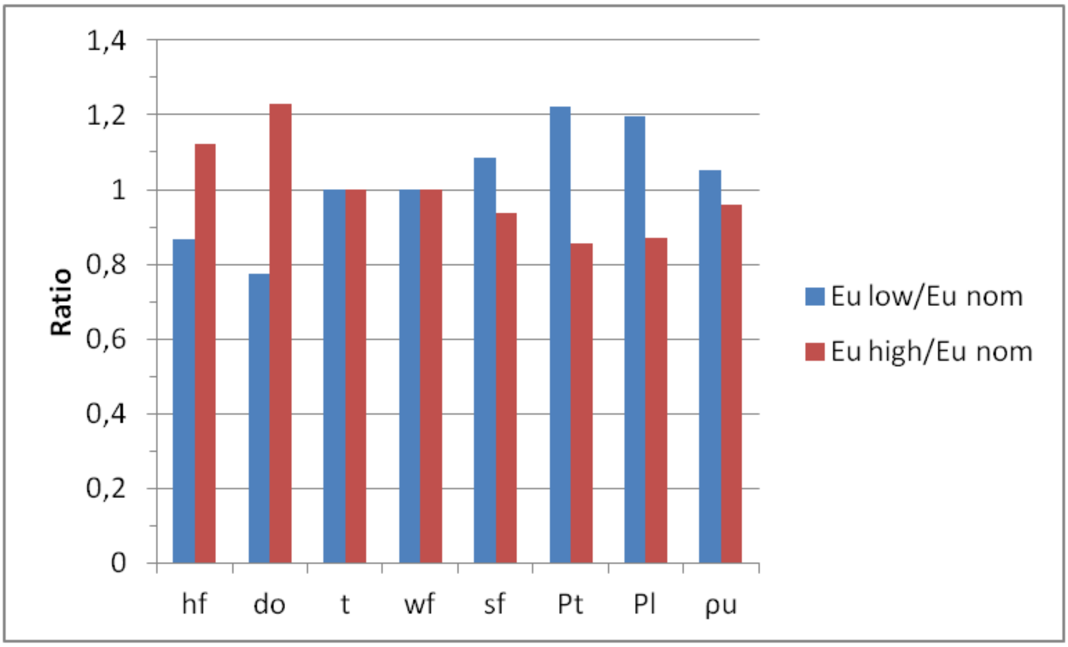

Figure 32 Sensitivity analysis pressure drop correlation for serrated fins (equation 40)

The two parameters P_t and P_t had a large impact on the Euler number. According to the analysis, an increase of these variables resulted in a significant decrease of the pressure drop. It was also observed that the Reynolds number was not as important as it was for the heat transfer coefficient. The increase of either the fin height or the tube outside diameter increased the Euler number, while an increase of the fin pitch decreased the Euler number.

The sensitivity analysis for the pressure drop correlation using Ar (equation 41) gave the results below:

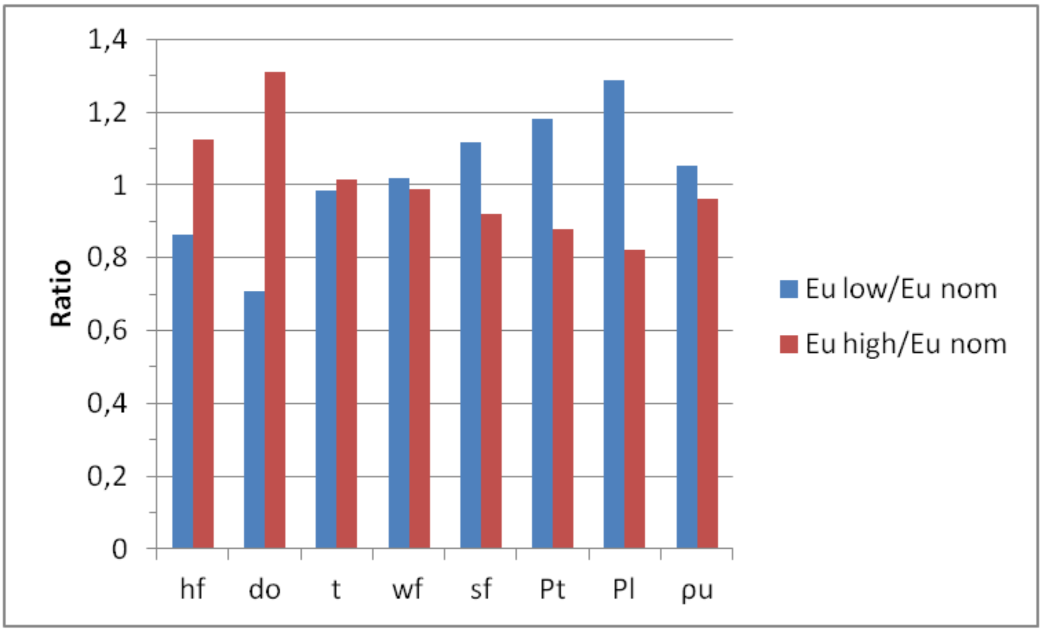

Figure 33 Sensitivity analysis for pressure drop correlation using Ar for serrated fins (equation 41)

The same things were observed for this correlation as in the first version. However, the increase in the longitudinal tube pitch decreased the Euler number even more than in the first correlation.

3.6.4 Pressure drop correlations for solid fins

The results from the sensitivity analysis of the pressure drop correlation using the different dimensionless groups for fin geometry (equation 47) and the pressure drop correlation using Ar (equation 48) are shown in the column diagrams below:

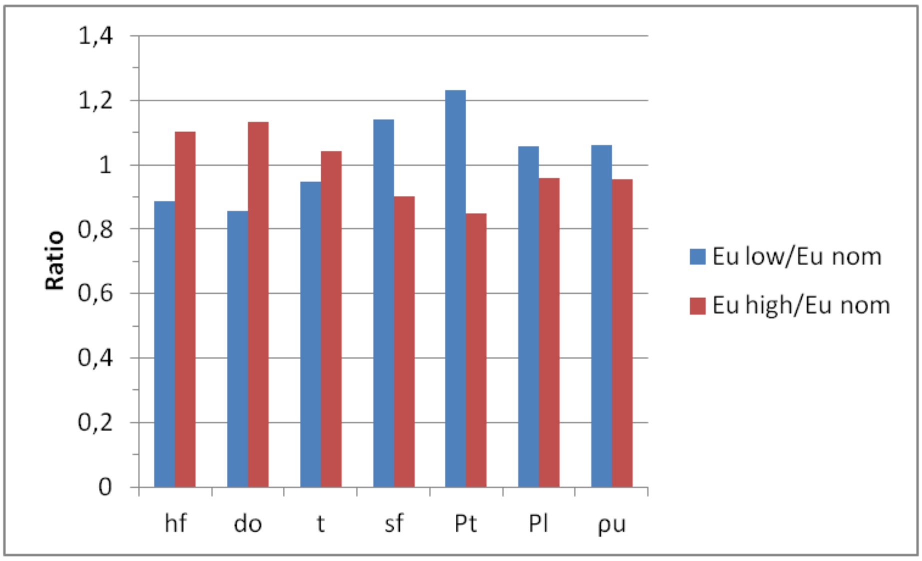

Figure 34 Sensitivity analysis of pressure drop correlation for solid fins (equation 47)

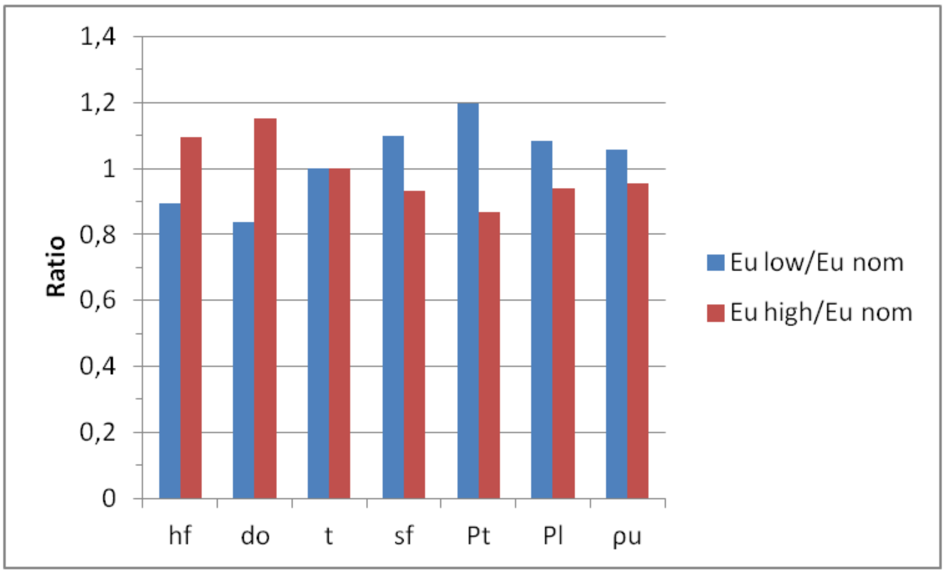

Figure 35 Sensitivity analysis of pressure drop correlation (using Ar) for solid fins (equation 48)

For both of the correlations, an increase in the transversal tube pitch gave a significant reduction in the Euler number. However, the decrease in the Euler number when increasing the longitudinal tube pitch was not as large as it was for the pressure drop correlations for serrated fins. Increasing either the fin height or the tube outside diameter led to a significant rise in pressure drop for both of the correlations. The pressure drop was reduced when the fin pitch was increased. The fin thickness did not affect the Euler number in the Ar correlation, but in the first correlation it was seen that increasing the fin thickness increased the Euler number slightly.

3.7 Effect of segment height

There are not many authors who have investigated the effect of the segment height on the heat transfer and the pressure drop. This is interesting for serrated I-foot fins, where there is a solid part and a segmented part.

Kawaguchi et al. (2006a) and Kawaguchi et al. (2006b) investigated how the pressure drop and the heat transfer changed when comparing two geometries (named SR211HK and SR211LK) that only differed in segment height. In addition a third geometry (SR210K) with a higher fin height (13,0 mm) than the two others (9,0 mm) was used. The table below presents the ratio between the segment height and the fin height for the three geometries:

Table 10 Ratio between segment height and fin height for the geometries

Geometry:	**SR210K**	**SR211HK**	**SR211LK**
h_s/h_f	0,4846	0,4888	0,2666

The heat transfer data for the three geometries are sketched in the figure below:

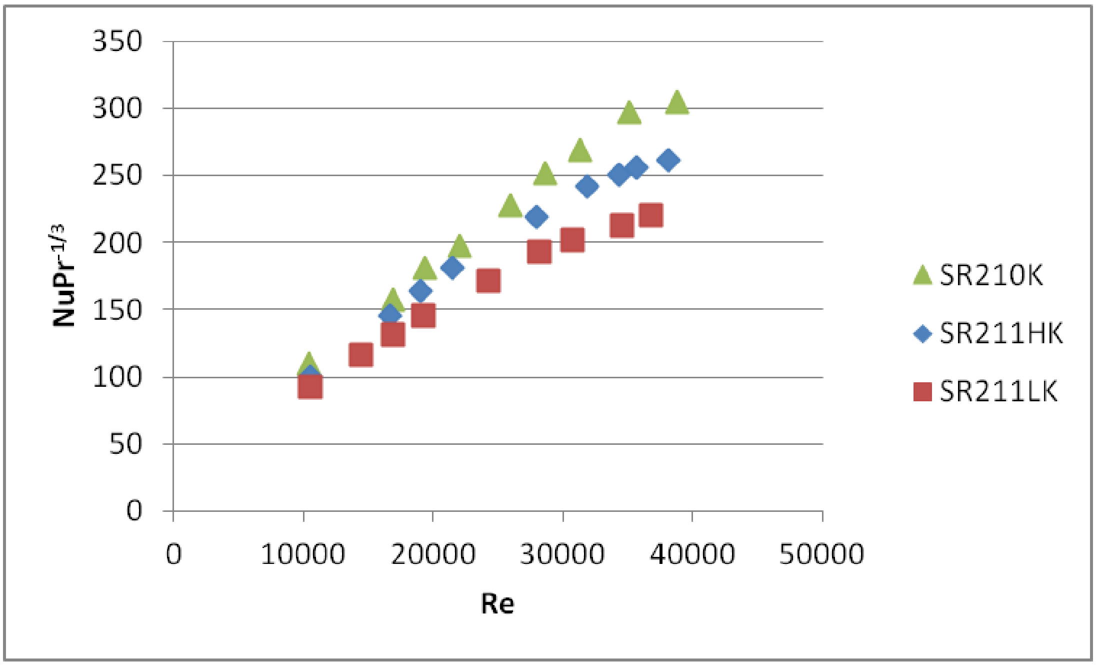

Figure 36 Comparison of the heat transfer data from Kawaguchi et al. (2006b)

The figure above shows that the geometry with the higher fin height had a higher heat transfer coefficient than the two other geometries. The two geometries that only differed in segment height had ca. the same heat transfer coefficient for the low Reynolds numbers, but for the higher Reynolds numbers it can be seen that the geometry with the highest segment height had ca. 15-20 % higher heat transfer coefficient than the one with the lower segment height.

A regression analysis using the heat transfer data for the three geometries was performed. The analysis led to the following regression equation:

$$Nu \cdot Pr^{-1/3} = 0{,}1224 \cdot Re^{0{,}7564} \cdot \left(\frac{h_s}{h_f}\right)^{0{,}30554} \quad (53)$$

Using only the data from the two geometries that differed in segment height (SR211HK and SR211LK) gave the regression equation below:

$$Nu \cdot Pr^{-1/3} = 0{,}1358 \cdot Re^{0{,}7347} \cdot \left(\frac{h_s}{h_f}\right)^{0{,}22} \quad (54)$$

Both of the equations above give the impression that the heat transfer coefficient will increase if the segment height is increased.

The pressure drop data for the same three geometries are sketched in the figure below:

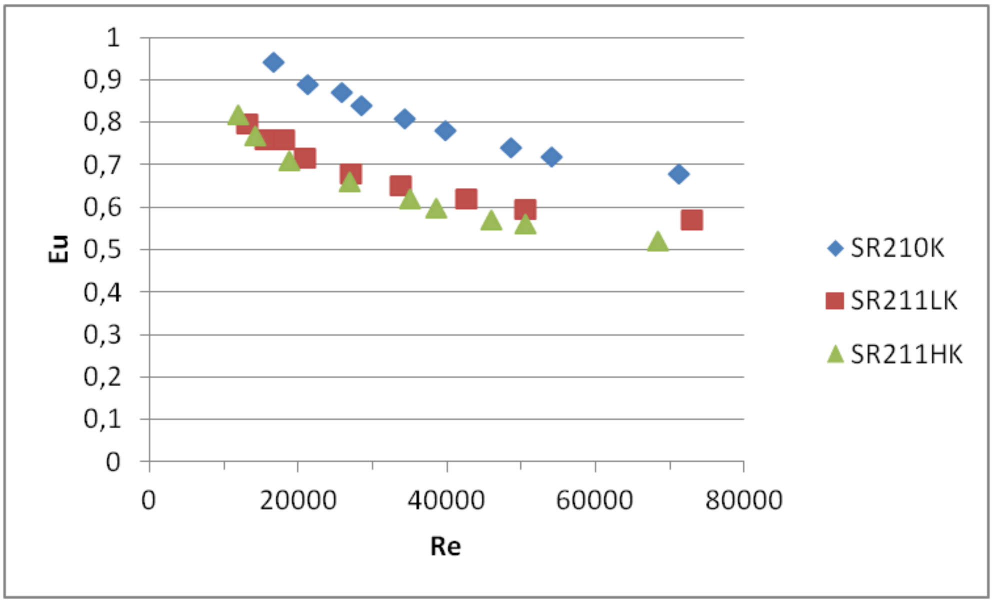

Figure 37 Comparison of the pressure drop data from Kawaguchi et al. (2006a)

It was observed that the geometry with a higher fin height had a higher pressure drop than the two geometries with a lower fin height. Comparing the two geometries that only differed in segment height, it was seen that the effect of the segment height was not very significant. The increase in segment height decreased the Euler number slightly.

The regression analysis using the pressure drop data for all the three geometries gave the following equation:

$$Eu = 6{,}6757 \cdot Re^{-0{,}20596} \cdot \left(\frac{h_s}{h_f}\right)^{0{,}1314} \tag{55}$$

The corresponding analysis using only the two geometries that differed only in segment height resulted in the equation below:

$$Eu = 6{,}444 \cdot Re^{-0{,}229} \cdot \left(\frac{h_s}{h_f}\right)^{-0{,}07377} \tag{56}$$

The effect of the segment height is opposite for the two equations; in the first equation an increase in segment height will increase the Euler number, while in the second equation the increase in segment height will decrease the Euler number. However, for both of the equations the effect of the segment height is rather low.

Conclusion: All in all the effect of the segment height was larger on the heat transfer coefficient than on the pressure drop.

3.7.1 Regression analysis of the heat transfer data for serrated and solid fins

In order to find out more about the effect of the segment height on the heat transfer coefficient, it was decided to use the data for both serrated and solid fins. However, only the data for those of the serrated fins that had I-foot fins were included, i.e. the geometries from Hashizume (1981), Kawaguchi et al. (2006b), Ma et al. (2011) and Weierman et al. (1978). It was also wished to include the data from Kawaguchi et al. (2005), but here the segment height was not given.

In order to find the dependency of the segment height, the following dimensionless group was used in the analysis:

$$\frac{h_f - h_s}{h_f} \tag{57}$$

Here, the value for the dimensionless group for solid fins always is equal to one (h_s=0 for solid fins).

From the inspection of all the data for F_t/F_d<1,0, it was observed that the data from Brauer (1964) should not be included (as in the regression analysis of the heat transfer data for solid fins, see chapter 3.4.3.2).

The regression analysis using all the data except from the data from Brauer (1964) resulted in the equation below:

$$Nu \cdot Pr^{-1/3} = 0{,}0497 \cdot Re^{0{,}7709} \cdot \left(\frac{P_t}{P_l}\right)^{-0{,}1673} \cdot \left(\frac{h_f - h_s}{h_f}\right)^{-0{,}286} \cdot \left(\frac{h_e}{s_f}\right)^{-0{,}3177} \cdot \left(\frac{d_f}{d_e}\right)^{0{,}764} \tag{58}$$

The exponent for P_t/P_l was not as expected, the heat transfer coefficient is expected to increase when the ratio P_t/P_l is increasing (the same observed in the regression analysis for heat transfer for solid fins, see chapter 3.4.3.2). For some reason the exponent changed sign when the data from Stasiulevicius et al. (1988) were removed before performing the analysis. The data from Hashizume (1981) and geometry 6 from Ward and Young (1959) were calculated too high using the equation above (30-50 % higher and 30-55 % higher respectively). Therefore these data were removed as well. The regression analysis for the remaining data gave the equation below:

$$Nu \cdot Pr^{-1/3} = 0{,}04 \cdot Re^{0{,}7917} \cdot \left(\frac{P_t}{P_l}\right)^{0{,}2603} \cdot \left(\frac{h_f - h_s}{h_f}\right)^{-0{,}35153} \cdot \left(\frac{h_e}{s_f}\right)^{-0{,}3459} \cdot \left(\frac{d_f}{d_e}\right)^{0{,}76627} \quad (59)$$

From the above equation, it is seen that an increase in the segment height will result in an increase of the heat transfer coefficient. This is in agreement with the conclusions from Kawaguchi et al. (2006b).

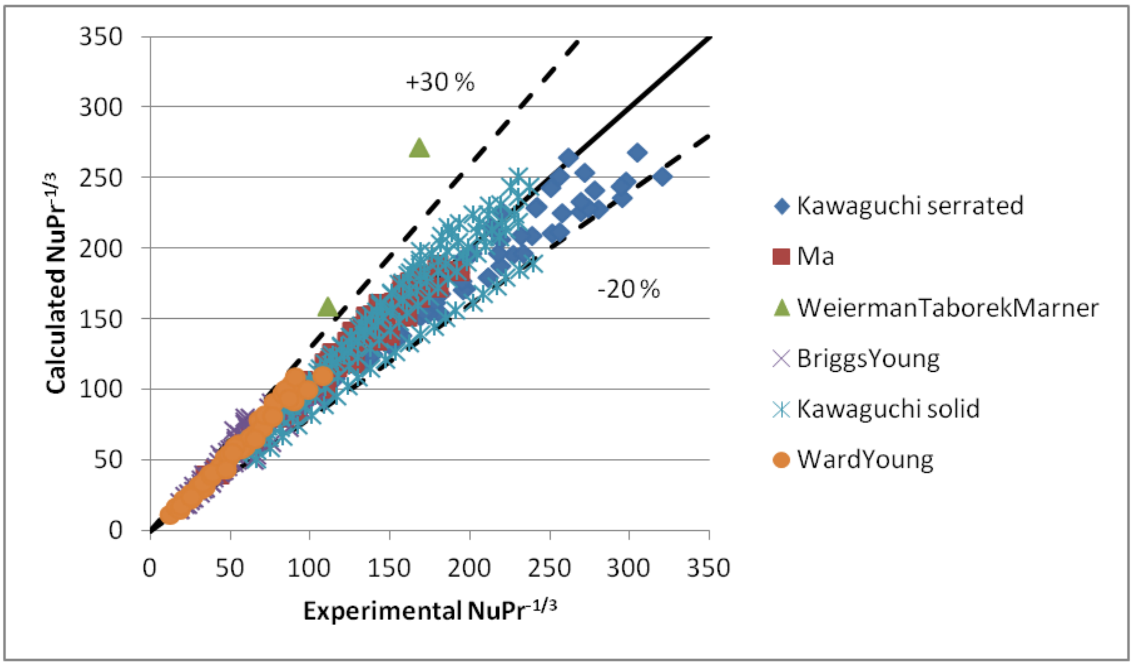

Figure 38 Prediction accuracy of the heat transfer correlation for both serrated and solid fins (eq. 59)

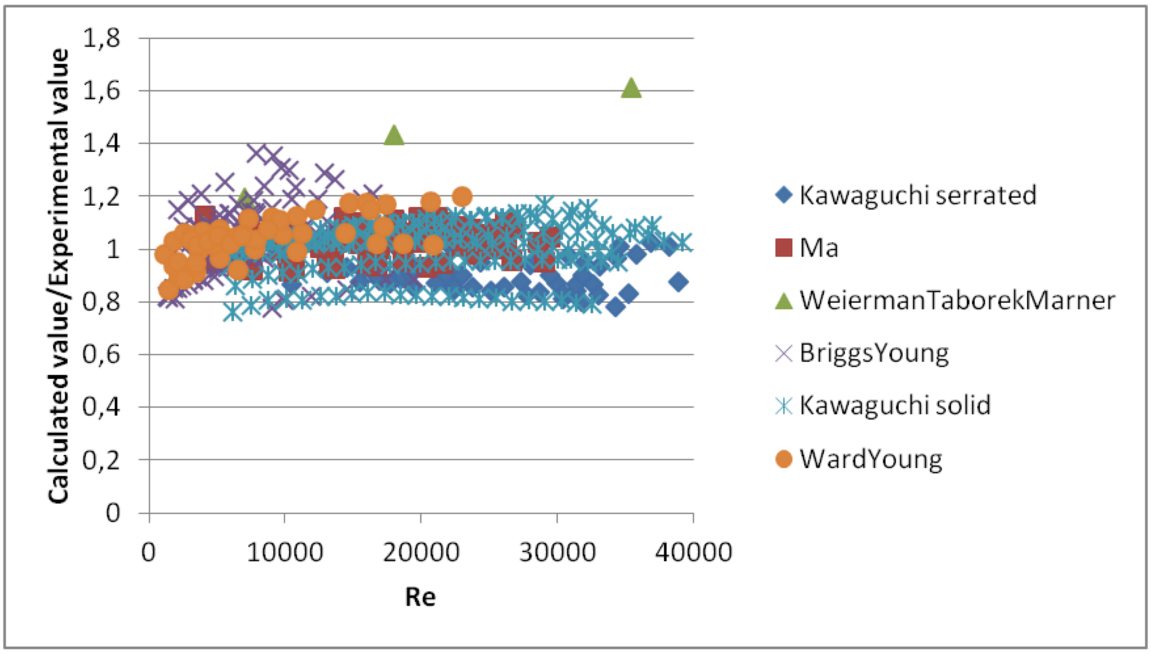

Figure 39 Ratio between calculated (eq. 59) and experimental value vs Re for serrated/solid correlation (heat transfer)

95,4 % of the data were predicted within ±20 %, 66,8 % of the data were predicted within ±10 %.

3.7.2 Regression analysis of the pressure drop data for serrated and solid fins

The regression analysis was also performed for the pressure drop data for both serrated and solid fins in order to find out how the segment height influenced the Euler number. Also in this case the data for those of the serrated fins that had I-foot fins were included. The following dimensionless group was used in order to find the dependency of the segment height (the same as in the analysis of the heat transfer data):

$$\frac{h_f - h_s}{h_f} \tag{57}$$

Only the data for Re<50 000 were included. In addition, Euler numbers larger than 1,2 for solid fins were not included (as the regression equation seemed to fail for the higher Euler numbers, see chapter 3.4.2.3).

When the regression analysis was performed for all the data, it was seen that the data from Hashizume (1981) were overestimated (calculated ca. 40 % higher than the experimental values). The same trend was observed for the data from Briggs and Young (1963) and geometry 5v from Brauer (1964).

Therefore the analysis was performed again without the data mentioned above in order to get a more accurate regression equation for the rest of the data. The analysis resulted in the following equation:

$$Eu = 6{,}37 \cdot Re^{-0{,}1926} \cdot \left(\frac{P_t}{d_e}\right)^{-0{,}7117} \cdot \left(\frac{P_l}{d_e}\right)^{-0{,}3224} \cdot \left(\frac{h_f - h_s}{h_f}\right)^{-0{,}08384} \cdot \left(\frac{h_e}{s_f}\right)^{0{,}23255} \cdot \left(\frac{d_f}{d_e}\right)^{0{,}4831} \tag{60}$$

The exponent for the dimensionless group $\frac{h_f - h_s}{h_f}$ is negative. In other words the correlation gives the impression that the Euler number increases when the segment height, h_s, is increased. This is contrary to the results from Kawaguchi et al. (2006a), where the Euler number was slightly higher for geometry SR211LK (h_s=2,4 mm) than for geometry SR211HK (h_s=4,4 mm). However, in general serrated fins have higher pressure drop than solid fins. This has been verified by the experiments from Weierman (1977).

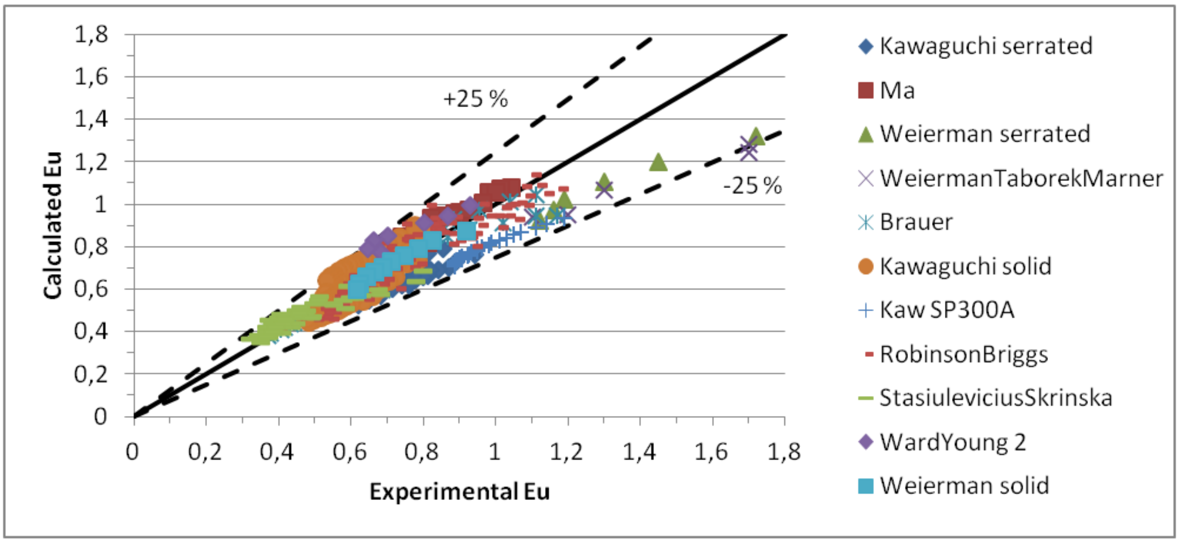

Figure 40 Prediction accuracy of the pressure drop correlation (eq. 60) for serrated/solid fins

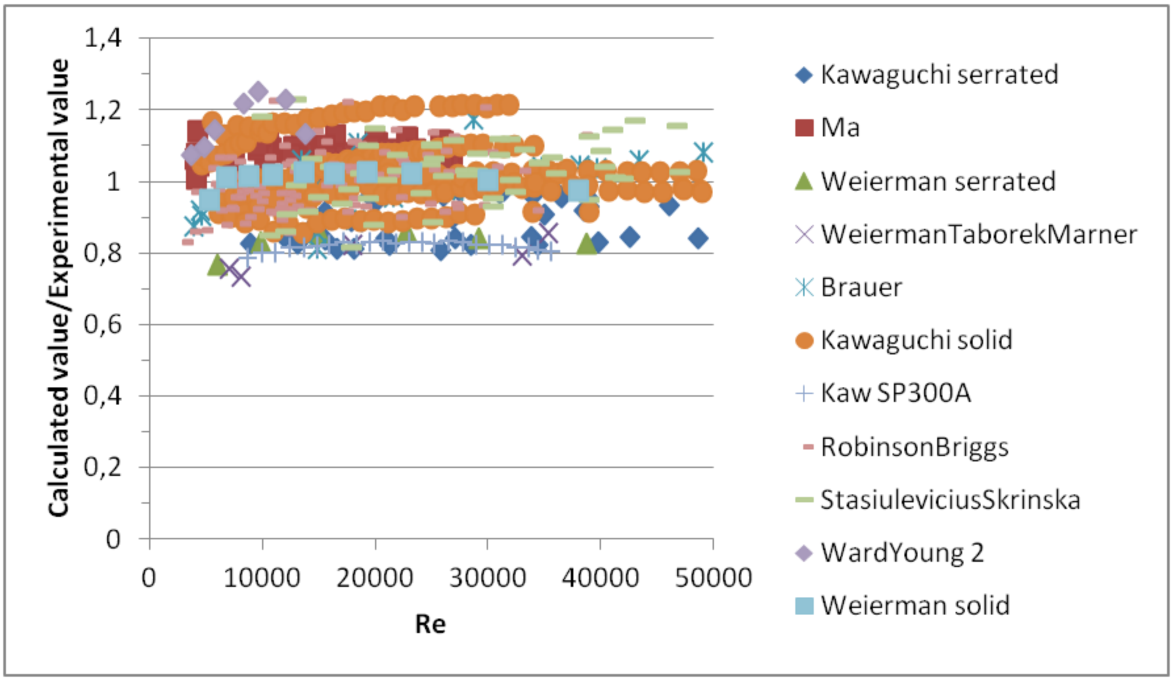

Figure 41 Ratio between calculated (eq. 60) and experimental value vs Re for serrated/solid correlation (pressure drop)

95,9 % of the data were predicted within ±20 %, while 69,3 % of the data were predicted within ±10 %. The data from Weierman (1977) (serrated fins) and Weierman et al. (1978) were estimated 15-25 % lower than the experimental value.

4 Summary, conclusions and recommendations for further work

4.1 Summary

The exhaust gas from gas turbines contains a large amount of heat that can be utilized for process purposes or for further power generation. The heat recovery units on offshore platforms are required to be as compact and light as possible. During the design of waste heat recovery units correlations are used to estimate the heat transfer and pressure drop. The correlations in the literature have limited validity ranges. The aim of this project was to develop correlations with a wider range of validity than the correlations in the literature. Data from different experimenters, collected in databases, were used in order to establish the new correlations.

The report can be divided into the following two parts:

1) Literature survey of multivariate analysis:

A literature survey of the method of multivariate analysis was done. Here the aim was to find a method that could be used in order to develop the new correlations. The multivariate method called multiple linear regression was chosen. In order to select which variables to include in the multiple linear regression, the variable selection procedure called best subsets regression was carried out. The regression analysis was performed with the statistical software Minitab 16.

2) Regression analysis:

The data from the two available databases for serrated and solid fins were used in the regression analysis. Correlations for heat transfer and pressure drop were developed for both serrated and solid fins. It was decided to develop two different versions for each correlation: The first version was using different dimensionless groups for fin geometry, while the second version was using Ar (defined by PFR (1976)) as fin geometry effect. For both versions the effect of the Reynolds number and the tube bundle layout was included. In addition, the effect of the segment height on the heat transfer and the pressure drop was investigated.

All the Minitab output from the regression analysis can be found in a separate attached file.

From the regression analysis of the heat transfer data for serrated fins the following correlations are recommended:

For $F_t/F_d<1,0$:

$$Nu \cdot Pr^{-1/3} = 0{,}0703 \cdot Re^{0{,}7404} \cdot \left(\frac{P_t}{d_e}\right)^{0{,}2359} \cdot \left(\frac{h_e}{s_f}\right)^{-0{,}20572} \cdot \left(\frac{d_f}{d_e}\right)^{0{,}5073} \qquad (25)$$

The correlation predicted 90,2 % of the data within ±20 %. 71,8 % of the data were predicted within ±10 %.

$$Nu \cdot Pr^{-1/3} = 0{,}0821 \cdot Re^{0{,}7396} \cdot \left(\frac{P_t}{d_e}\right)^{0{,}2902} \cdot Ar^{-0{,}0697} \qquad (35)$$

The regression equation predicted 98,4 % of the data within ±20 % . 81,2 % of the data were predicted within ±10 %.

For $F_t/F_d>1,0$:

$$Nu \cdot Pr^{-1/3} = 0{,}1539 \cdot Re^{0{,}7404} \cdot \left(\frac{h_e}{s_f}\right)^{-0{,}20572} \cdot \left(\frac{d_f}{d_e}\right)^{0{,}5073} \cdot \left(\frac{P_t}{P_l}\right)^{-0{,}7726} \qquad (37)$$

The correlation predicted all the data from +10 % to -12 %.

$$Nu \cdot Pr^{-1/3} = 0{,}1698 \cdot Re^{0{,}7396} \cdot \left(\frac{P_t}{P_l}\right)^{-0{,}60923} \cdot Ar^{-0{,}0697} \qquad (39)$$

The correlation predicted all the data from +12 % to -14 %.

From the regression analysis of the pressure drop data for serrated fins, the following correlations are recommended:

For $F_t/F_d<1,0$:

$$Eu = 7{,}132 \cdot Re^{-0{,}1775} \cdot \left(\frac{P_t}{d_e}\right)^{-0{,}6928} \cdot \left(\frac{P_l}{d_e}\right)^{-0{,}623} \cdot \left(\frac{h_e}{s_f}\right)^{0{,}2827} \cdot \left(\frac{d_f}{d_e}\right)^{0{,}4954} \tag{40}$$

The equation predicted 96,4 % of the data within ±20 %. 73,8 % of the data were predicted within ±10 %.

$$Eu = 5{,}867 \cdot Re^{-0{,}1804} \cdot \left(\frac{P_t}{d_e}\right)^{-0{,}58387} \cdot \left(\frac{P_l}{d_e}\right)^{-0{,}88026} \cdot Ar^{0{,}4153} \tag{41}$$

98,5 % of the data were predicted within ±20 %, while 75,9 % of the data were predicted within ±10 %.

From the regression analysis of the heat transfer data for solid fins the following correlations are recommended (for $F_t/F_d<1,0$):

$$Nu \cdot Pr^{-1/3} = 0{,}117 \cdot Re^{0{,}659} \cdot \left(\frac{P_t}{P_l}\right)^{0{,}24502} \cdot \left(\frac{h_f}{s_f}\right)^{-0{,}21808} \cdot \left(\frac{d_f}{d_e}\right)^{0{,}29684} \cdot \left(\frac{s_f}{t}\right)^{0{,}11758} \tag{45}$$

93,9 % of the data were predicted within ±20 %. 80,8 % of the data were predicted within ±10 %.

$$Nu \cdot Pr^{-1/3} = 0{,}176 \cdot Re^{0{,}652} \cdot \left(\frac{P_t}{P_l}\right)^{0{,}3667} \cdot Ar^{-0{,}0969} \tag{46}$$

93 % of the data were predicted within ±20 %. 65,7 % of the data were predicted within ±10 %.

From the regression analysis of the pressure drop data for solid fins the following correlations are recommended (For F_t/F_d<1,0):

$$Eu = 9{,}82 \cdot Re^{-0{,}20979} \cdot \left(\frac{P_t}{d_e}\right)^{-0{,}72394} \cdot \left(\frac{P_l}{d_e}\right)^{-0{,}19613} \cdot \left(\frac{h_f}{s_f}\right)^{0{,}2634} \cdot \left(\frac{t}{s_f}\right)^{0{,}19259} \cdot \left(\frac{d_f}{d_e}\right)^{0{,}3971} \tag{47}$$

98 % of the data were predicted within ±20 %, while 70,8 % of the data were predicted within ±10 %.

$$Eu = 4{,}817 \cdot Re^{-0{,}1976} \cdot \left(\frac{P_t}{d_e}\right)^{-0{,}626} \cdot \left(\frac{P_l}{d_e}\right)^{-0{,}28395} \cdot Ar^{0{,}34595} \tag{48}$$

95,3 % of the data were predicted within ±20 %, while 68,4 % of the data were predicted within ±10 %.

4.2 Conclusions

The analysis of the heat transfer data gave the following conclusions:

The main parameter influencing the heat transfer coefficient was the gas flow rate. The tube bundle layout had a larger impact on the heat transfer coefficient than the fin geometry. This was the case for both serrated and solid fins. The transversal tube pitch had a significant effect on the heat transfer coefficient for $F_t/F_d<1,0$. The increase in transversal tube pitch increased the heat transfer coefficient for both serrated and solid fins. The longitudinal tube pitch did not have any significant effect on the heat transfer coefficient in the same range for serrated fins. For solid fins, the heat transfer coefficient tended to decrease when the longitudinal tube pitch was increased for $F_t/F_d<1,0$.

For $F_t/F_d>1,0$, the effect of both of the tube bundle layout variables was significant for serrated fins. The heat transfer coefficient seemed to reach its maximum for ca. $F_t/F_d=1,0$. After this the heat transfer coefficient decreased monotonically when the ratio P_t/P_l was increased.

The heat transfer coefficient (for both serrated and solid fins) was also influenced by the following parameters:

- Tube outside diameter: The increase of the tube outside diameter increased the heat transfer coefficient.
- Fin pitch: Increasing the fin pitch increased the heat transfer coefficient.

The analysis of the pressure drop data gave the following conclusions:

For the pressure drop data it was observed that the tube bundle layout had a very large impact on the Euler number. Increasing the transversal or the longitudinal tube pitch decreased the Euler number significantly. However, the effect of the longitudinal tube pitch on the Euler number was larger for serrated fins than for solid fins.

The Euler number was also influenced by the following parameters:

- Tube outside diameter: Increasing the tube outside diameter increased the pressure drop.
- Fin pitch: Increasing the fin pitch led to an increase in pressure drop.

- Fin height: The increase in fin height increased the pressure drop.

In addition the increase in segment height increased both the heat transfer coefficient and the pressure drop, but this should be verified by further experiments.

4.3 Recommendations for further work

For serrated fins there are available data for heat transfer and pressure drop for both ranges $F_t/F_d<1,0$ and $F_t/F_d>1,0$. However, there is a very limited amount of data for the range $F_t/F_d>1,0$, i.e. where the minimum free-flow area is in the diagonal plane. Actually, only the seven geometries tested by Næss (2007) cover this range. The change of tube bundle layout dependency for $F_t/F_d=1,0$ found by Næss (2007) should be verified by further experiments. In the correlations developed in this project, the fin geometry effect is assumed to be the same for both of the ranges. As pointed out by Næss (2007), this should be verified by further experiments in the range $F_t/F_d>1,0$.

All the available heat transfer and pressure drop data for solid fins are in the range $F_t/F_d<1,0$, therefore it is also recommended to perform experiments in the range $F_t/F_d>1,0$ for solid fins.

Kawaguchi et al. (2006b) investigated the effect of varying only the segment height on the pressure drop, while the effect on the heat transfer was investigated in Kawaguchi et al. (2006a). However, these reports seem like the only ones that investigate the effect of only varying the segment height. More experiments using geometries only differing in segment height are therefore suggested.

The effect of varying only the fin segment width, w_f, is not investigated in the available literature. According to Næss (2007) the segment width will influence the thickness of the boundary layers which especially will affect the heat transfer coefficient. The investigation of geometries differing only in segment width could be considered.

In this project only data for staggered tube layouts have been used in the analysis. However, in the database implemented by Kaspersen (1995) there are also data for in-line tube layouts. Performing the similar analysis as in this project for the in-line tube layout data is possible. The heat transfer coefficient and the Euler number was observed to be higher for staggered tube layout than for in-line tube layout by Weierman et al. (1978) and Ackerman and Brunsvold (1970). It should be noted that there is a rather small amount of data for in-line tube layouts in the literature, so more experimental measurements in in-line tube layouts could be performed.

In the database for solid fins only data for staggered tube layouts have been collected. One possibility is therefore to collect data for in-line tube layouts as well. However, according to Næss (2010) the in-line tube layouts are generally less compact than staggered tube layouts. Therefore a further investigation of in-line tube layouts probably will be more useful for onshore applications.

Appendix A Correlations from the available literature

Table A-1 Heat transfer correlations for serrated fins

Author	Correlation
Weierman (McKetta (1992))	$Nu = 0{,}25 \cdot Re^{0,65} \cdot Pr^{1/3} \cdot \left\{0{,}55 + 0{,}45 \cdot e^{\left(-0{,}35 \cdot \frac{h_f}{s}\right)}\right\} \cdot \left\{0{,}7 + \left(0{,}7 - 0{,}8 \cdot e^{\left(-0{,}15 \cdot N_l^2\right)}\right) \cdot e^{-\frac{P_l}{P_t}}\right\} \cdot \left(\frac{d_f}{d_o}\right)^{0,5} \cdot [T_b/T_s]^{0,25}$
Worley and Ross (1960)	$Nu = 0{,}125 \cdot Re^{0,7} \cdot Pr^{1/3}$
Biraghi (Kaspersen (1995))	$Nu = 0{,}414 \cdot Re^{0,588} \cdot Pr^{1/3}$
Ackerman and Brunsvold (1970)	$Nu = 0{,}497 \cdot Re^{0,547} \cdot Pr^{1/3} \cdot \left(\frac{P_t}{d_o}\right)^{0,34}$
ESCOA (Næss (2007))	$Nu = 0{,}091 \cdot Re^{0,75} \cdot Pr^{1/3} \cdot \left\{0{,}35 + 0{,}65 \cdot e^{\left(-0{,}17 \cdot \frac{h_f}{s_f}\right)}\right\} \cdot \left\{0{,}7 + \left(0{,}7 - 0.8 \cdot e^{\left(-0{,}15 \cdot N_l^2\right)}\right) \cdot e^{-\frac{P_l}{P_t}}\right\} \cdot \left(\frac{d_f}{d_o}\right)^{0,5} \cdot [T_b/T_s]^{0,25}$
Hofmann (2009)	$Nu = 0{,}36475 \cdot Re^{0,6013} \cdot Pr^{1/3} \cdot \left[1 - 0{,}392 \cdot log\left(\frac{N_{l,\infty}}{N_l}\right)\right]$
Ma et al. (2011)	$Nu = 0{,}117 \cdot Re^{0,717} \cdot Pr^{0,33} \cdot \left(0{,}6 + 0{,}4 \cdot e^{-\frac{250 \cdot h_{f/s}}{Re}}\right) \cdot \left(\frac{P_t}{P_l}\right)^{0,06}$
Næss (2010)	$Nu = 0{,}107 \cdot Re^{0,65} \cdot Pr^{1/3} \cdot \left(\frac{h_e}{s_f}\right)^{-0,14} \cdot \left(\frac{s_f}{d_e}\right)^{-0,2} \cdot \left(\frac{P_t}{d_e}\right)^{0,35} \cdot \left(\frac{h_e}{d_e}\right)^{-0,13}$
PFR (1976)	$Nu = 0{,}195 \cdot Re^{0,7} \cdot Pr^{1/3} \cdot Ar^{-0,17}$

Table A-2 Heat transfer correlations for solid fins

Author	Correlation
Briggs and Young (1963)	$Nu = 0{,}134 \cdot Re^{0{,}681} \cdot Pr^{1/3} \cdot \left(\frac{s}{h_f}\right)^{0{,}2} \cdot \left(\frac{s}{t}\right)^{0{,}1134}$
Stasiulevicius et al. (1988)	$Nu = 0{,}044 \cdot \left(\frac{P_t}{P_l}\right)^{0{,}2} \cdot \left(\frac{s_f}{d_o}\right)^{0{,}18} \cdot \left(\frac{h_f}{d_o}\right)^{-0{,}14} \cdot Re^{0{,}8}$
Ward and Young (1959)	$Nu = 0{,}364 \cdot Re^{0{,}68} \cdot Pr^{1/3} \cdot \left(\frac{d_f}{d_o}\right)^{0{,}45} \cdot \left(\frac{t}{d_f}\right)^{0{,}3}$
PFR (1976)	$Nu = 0{,}29 \cdot Re^{0{,}633} \cdot Pr^{1/3} \cdot Ar^{-0{,}17}$
Schmidt (Mon (2003))	$Nu = 0{,}45 \cdot Re^{0{,}625} \cdot Pr^{1/3} \cdot \left(\frac{A}{A_t}\right)^{-0{,}375}$
VDI (1997)	$Nu = 0{,}38 \cdot Re^{0{,}6} \cdot Pr^{1/3} \cdot \left(\frac{A}{A_t}\right)^{-0{,}15}$
Weierman (McKetta (1992))	$Nu = 0{,}25 \cdot Re^{0{,}65} \cdot Pr^{1/3} \cdot \left\{0{,}35 + 0{,}65 \cdot e^{\left(-0{,}25 \cdot \frac{h_f}{s}\right)}\right\} \cdot \left\{0{,}7 + \left(0{,}7 - 0{,}8 \cdot e^{\left(-0{,}15 \cdot N_l^2\right)}\right) \cdot e^{-\frac{P_l}{P_t}}\right\} \cdot \left(\frac{d_f}{d_o}\right)^{0{,}5} \cdot [T_b/T_s]^{0{,}25}$

Table A-3 Pressure drop correlations for serrated fins

Author	**Correlation**
Biraghi (Kaspersen (1995))	$Eu = 2{,}892 \cdot Re^{-0{,}137}$
Weierman (McKetta (1992))	$$Eu = \left\{0{,}28 + \frac{32}{Re^{0{,}45}}\right\} \cdot \left\{0{,}11 \cdot \left[0{,}05 \cdot \frac{P_t}{d_o}\right]^{-0{,}7 \cdot \left(\frac{h_f}{s}\right)^{0.23}}\right\} \cdot \left\{1{,}1 + \left(1{,}8 - 2{,}1 \cdot e^{-0{,}15 \cdot {N_l}^2}\right) \cdot e^{-2 \cdot \frac{P_l}{P_t}} - \left(0{,}7 - 0{,}8 \cdot e^{(-0{,}15 \cdot {N_l}^2)}\right) \cdot e^{-0{,}6 \cdot \frac{P_l}{P_t}}\right\} \cdot \left(\frac{d_f}{d_o}\right)^{0{,}5}$$
Næss (2010)	$$Eu = \left[0{,}24 + \frac{8{,}2}{Re^{0{,}5}}\right] \cdot \left(\frac{h_e}{d_e}\right)^{0{,}18} \cdot \left(\frac{s_f}{d_e}\right)^{-0{,}74} \cdot min\left(1{,}0 \,; 0{,}52 + 964{,}5 \cdot e^{-3{,}24 \cdot \frac{P_t}{P_l}}\right)$$
Ma et al. (2011)	$$Eu = 3{,}546 \cdot Re^{-0{,}184} \cdot \left(\frac{h_f}{s}\right)^{0{,}556} \cdot \left(\frac{P_t}{d_o}\right)^{-0{,}673} \cdot \left(\frac{P_l}{d_o}\right)^{-0{,}133}$$
Kawaguchi et al. (2006a)	$$Eu = \frac{4{,}99}{{Re_{d_h}}^{0{,}23}} \cdot \left(\frac{h_f}{d_h}\right)^{0{,}13} \cdot \left(\frac{s_f - t}{s_f}\right)^{-1{,}19}$$

Table A-4 Pressure drop correlations for solid fins

Author	Correlation
Weierman (McKetta (1992))	$$Eu = \left\{0,28 + \frac{32}{Re^{0,45}}\right\} \cdot \left\{0,11 \cdot \left[0,05 \cdot \frac{P_t}{d_o}\right]^{-0,7 \cdot \left(\frac{h_f}{s}\right)^{0.2}}\right\} \cdot \left\{1,1 + \left(1,8 - 2,1 \cdot e^{-0,15 \cdot N_l^2}\right) \cdot e^{-2 \cdot \frac{P_l}{P_t}} - \left(0,7 - 0,8 \cdot e^{(-0,15 \cdot N_l^2)}\right) \cdot e^{-0,6 \cdot \frac{P_l}{P_t}}\right\} \cdot \left(\frac{d_f}{d_o}\right)^{0,5}$$
Stasiulevicius et al. (1988)	$$Eu = \frac{13,1 \cdot \left(1 - \frac{s_f}{d_o}\right)^{1,8} \cdot Re^{-0,25}}{\left(\frac{P_t}{d_0}\right)^{0,55} \cdot \left(\frac{P_l}{d_o}\right)^{0,5} \cdot \left(1 - \frac{h_f}{d_o}\right)^{1,4}}$$
Robinson and Briggs (1966)	$$Eu = 37,86 \cdot Re^{-0,316} \cdot \left(\frac{P_t}{d_o}\right)^{-0,927} \cdot \left(\frac{P_t}{P_x}\right)^{0,515}$$
Ward and Young (Mon (2003))	$$Eu = 0,512 \cdot Re^{-0,264} \cdot \left(\frac{t}{d_f}\right)^{-0,377} \cdot \left(\frac{s}{d_o}\right)^{-0,396} \cdot \left(\frac{P_l}{d_o}\right)$$

Appendix B More correlations from the regression analysis

In this appendix the correlations from the regression analysis that were not presented/recommended in chapter 3.4 will be presented. Basically, these are the correlations that were developed in the steps before the recommended ones. In the left column, the data which the correlations are developed for are presented.

Table A-5 Heat transfer correlations for serrated fins from the regression analysis

Data	Correlation
All, F_t/F_d<1,0	$Nu \cdot Pr^{-1/3} = 0{,}124 \cdot Re^{0{,}7033} \cdot \left(\frac{P_t}{P_l}\right)^{0{,}2137} \cdot \left(\frac{h_e}{s_f}\right)^{-0{,}19451} \cdot \left(\frac{d_f}{d_e}\right)^{0{,}4679}$
All, F_t/F_d<1,0	$Nu \cdot Pr^{-1/3} = 0{,}177 \cdot Re^{0{,}68} \cdot \left(\frac{P_t}{P_l}\right)^{0{,}351} \cdot Ar^{-0{,}0512}$
All, F_t/F_d<1,0 (Ar calculated as for solid fins)	$Nu \cdot Pr^{-1/3} = 0{,}203 \cdot Re^{0{,}694} \cdot \left(\frac{P_t}{P_l}\right)^{0{,}27881} \cdot Ar_{sol}{}^{-0{,}13891}$
All except from Cox (1973) and Schryber (1945), F_t/F_d<1,0. (Ar calculated as for solid fins)	$Nu \cdot Pr^{-1/3} = 0{,}104 \cdot Re^{0{,}7412} \cdot \left(\frac{P_t}{d_e}\right)^{0{,}28496} \cdot Ar_{sol}{}^{-0{,}14814}$

Table A-6 Heat transfer correlations for solid fins from regression analysis

Data	Correlation
All except from the geometries 5v, 6v, 7v, 8v and 9v from Brauer (1964)	$Nu \cdot Pr^{-1/3} = 0{,}0756 \cdot Re^{0{,}7924} \cdot \left(\frac{P_t}{P_l}\right)^{-0{,}19185} \cdot Ar^{-0{,}19918}$
All except from the data from Brauer (1964) and Stasiulevicius et al. (1988)	$Nu \cdot Pr^{-1/3} = 0{,}0475 \cdot Re^{0{,}76896} \cdot \left(\frac{P_t}{P_l}\right)^{0{,}37087} \cdot \left(\frac{h_f}{s_f}\right)^{-0{,}33038} \cdot \left(\frac{d_f}{d_e}\right)^{0{,}75496}$
All except from the data from Brauer (1964) and Stasiulevicius et al. (1988)	$Nu \cdot Pr^{-1/3} = 0{,}0452 \cdot Re^{0{,}81939} \cdot \left(\frac{P_t}{d_e}\right)^{0{,}25938} \cdot Ar^{-0{,}18483}$

Table A-7 Pressure drop correlations for serrated fins from regression analysis

Data	Correlation
Only data from authors with six or more data points (see chapter 3.4.2.3), Ar calculated as for solid fins, $F_t/F_d<1{,}0$	$Eu = 5{,}364 \cdot Re^{-0{,}1721} \cdot \left(\frac{P_t}{d_e}\right)^{-0{,}63537} \cdot \left(\frac{P_l}{d_e}\right)^{-0{,}65401} \cdot Ar_{sol}^{0{,}3605}$
All the data for $F_t/F_d>1{,}0$. Fin geometry effect kept from equation 41	$Eu = 41{,}34 \cdot Re^{-0{,}1804} \cdot \left(\frac{P_t}{d_e}\right)^{-2{,}77964} \cdot \left(\frac{P_l}{d_e}\right)^{1{,}02598} \cdot Ar^{0{,}4153}$

Table A-8 Pressure drop correlations for solid fins from regression analysis

Data	Correlation
All for Re<50 000	$Eu = 8{,}49 \cdot Re^{-0{,}2069} \cdot \left(\frac{P_t}{d_e}\right)^{-0{,}66356} \cdot \left(\frac{P_l}{d_e}\right)^{-0{,}2934} \cdot \left(\frac{h_f}{s_f}\right)^{0{,}2572} \cdot \left(\frac{t}{s_f}\right)^{0{,}0627} \cdot \left(\frac{d_f}{d_e}\right)^{0{,}2516}$
All for Re<50 000, using Ar	$Eu = 5{,}33 \cdot Re^{-0{,}202} \cdot \left(\frac{P_t}{d_e}\right)^{-0{,}62361} \cdot \left(\frac{P_l}{d_e}\right)^{-0{,}32347} \cdot Ar^{0{,}32398}$

References

Ackerman, J. and A. R. Brunsvold (1970). "Heat transfer and draft loss performance of extended surface tube banks." Journal of Heat Transfer **92**: 215-220.

Alvin, C. R. (2002). "Methods of multivariate analysis." Wiley Interscience.

Brauer, H. (1964). "Compact heat exchangers." Chem. Process Eng **45**(8): 451-460.

Briggs, D. E. and E. H. Young (1963). Convection heat transfer and pressure drop of air flowing across triangular pitch banks of finned tubes. Chem. Eng. Prog. Symp. Ser.

Chatterjee, S. and A. S. Hadi (2006). Regression analysis by example, Wiley-Interscience.

Cox, B. (1973). Heat transfer and pumping power performance in tube banks: finned and bare, Oak Ridge Gaseous Diffusion Plant, Tenn.(USA).

Der, G. and B. S. Everitt (2012). Applied medical statistics using SAS, CRC PressINC.

Esbensen, K. H., D. Guyot, F. Westad and L. P. Houmøller (2002). Multivariate data analysis-in practice: An introduction to multivariate data analysis and experimental design, Multivariate Data Analysis.

Feten, T. G. (2012). Heat exchangers for offshore gas turbines. Trondheim, Norges teknisk-naturvitenskapelige universitet.

Hashizume, K. (1981). "Heat transfer and pressure drop characteristics of finned tubes in cross flow." Heat Transfer Engineering **3**(2): 15-20.

Hofmann, R. (2009). Experimental and Numerical Gas-side Performance Evaluation of Finned Tube Heat Exchangers. Faculty of Mechanical and Industrial Engineering. Vienna, Austria, Technical University Vienna.

Kasai, K. (1998). "Soft tissue adaptability to hard tissues in facial profiles." American journal of orthodontics and dentofacial orthopedics **113**(6): 674-684.

Kaspersen, T. (1995). Varmeovergang og trykktap på gassiden i en avgassdampkjele. Trondheim, Norges Tekniske Høgskole.

Kawaguchi, K., K. Okui, T. Asai and Y. Hasegawa (2006a). "The heat transfer and pressure drop characteristics of finned tube banks in forced convection (effects of fin height on pressure drop characteristics)." Heat Transfer—Asian Research **35**(3): 179-193.

Kawaguchi, K., K. Okui, T. Asai and Y. Hasegawa (2006b). "The heat transfer and pressure drop characteristics of the finned tube banks in forced convection (effects of fin height on heat transfer characteristics)." Heat Transfer—Asian Research **35**(3): 194-208.

Kawaguchi, K., K. Okui and T. Kashi (2004). "The heat transfer and pressure drop characteristics of finned tube banks in forced convection (comparison of the pressure drop characteristics of spiral fins and serrated fins)." Heat Transfer—Asian Research **33**(7): 431-444.

Kawaguchi, K., K. Okui and T. Kashi (2005). "Heat transfer and pressure drop characteristics of finned tube banks in forced convection (comparison of the heat transfer characteristics between spiral fin and serrated fin)." Heat Transfer—Asian Research **34**(2): 120-133.

Larose, D. T. (2006). Data Mining Methods and Models, Wiley.

Lee, D. A. and K. Cincotta (2007). "The Multicollinearity Problem: Coping with the Persistent Beast."

Ma, Y., Y. Yichao, L. Yuzheng and H. Xiaohong (2011). "Experimental investigation of heat transfer and pressure drop in serrated finned tube banks with staggered layouts." Applied Thermal Engineering **37**: 314-323.

McKetta, J. J. (1992). Heat Transfer Design Methods, Marcel Dekker.

Mon, M. S. (2003). Numerical Investigation of Air-Side Heat Transfer and Pressure Drop in Circular Finned-Tube Heat Exchangers, Ph. D. Thesis, Technische Universität Bergakademie Freiberg, Freiberg, Germany.

Næss, E. (2007). An experimental study of heat transfer and pressure drop in serrated-fin tube bundles and investigation of particulate fouling in waste heat recovery heat exchangers. Trondheim, Norges teknisk-naturvitenskapelige universitet.

Avhandling (dr.ing.) - Norges teknisk-naturvitenskapelige universitet, Trondheim, 2007

Næss, E. (2010). "Experimental investigation of heat transfer and pressure drop in serrated-fin tube bundles with staggered tube layouts." Applied Thermal Engineering **30**(13): 1531-1537.

PFR (1976). Heat Transfer and Pressure Drop Characteristics of Dry Tower Extended Surfaces: Data analysis and correlation. PFR Report BNWL-PFR-7-100, Pacific Northwest Laboratory.

Rabas, T. and P. Eckels (1975). "Heat transfer and pressure drop performance of segmented extended surface tube bundles." ASME paper(75-HT): 45.

Robinson, K. K. and D. E. Briggs (1966). Pressure drop of air flowing across triangular pitch banks of finned tubes. Chem. Eng. Prog. Symp. Ser.

Schryber, E. (1945). "Heat Transfer Coefficients and Other Data on Individual Serrated-finned Surface." Transactions of the ASME **67**: 683-686.

Stasiulevicius, J., A. Skrinska and A. Zukauskas (1988). "Heat transfer of finned tube bundles in crossflow."

Stine, R. A. (1995). "Graphical interpretation of variance inflation factors." The American Statistician **49**(1): 53-56.

Vampola, J. (1966). "Heat transfer and pressure drop in flow of gases across finned tube banks." Strojiren-stvi **7**: 501-507.

VDI, W. (1997). Berechnungsblätter für den Wärmeübergang, Springer Verlag, Berlin Heidelberg.

Walpole, R., H. Myers, L. Myers and K. Ye (2007). Probability & statistics for engineers & scientists, Person Education, Inc.

Ward, D. J. and E. Young (1959). "Heat transfer and pressure drop of air in forced convection across triangular pitch banks of finned tubes." Chem. Eng. Progr. **55**.

Weierman, C. (1977). "Pressure drop data for heavy-duty finned tubes." Chemical engineering progress **73**(2): 69-72.

Weierman, C., J. Taborek and W. J. Marner (1978). "Comparison of the Performance of In-Line and Staggered Banks of Tubes With Segmented Fins." AIChE Symp. Ser. **74**: 39-46.

Whittingham, M. J., P. A. Stephens, R. B. Bradbury and R. P. Freckleton (2006). "Why do we still use stepwise modelling in ecology and behaviour?" Journal of Animal Ecology **75**(5): 1182-1189.

Worley, N. G. and W. Ross (1960). "Heat transfer and Pressure Loss Characteristics of Crossflow Tubular Arrangements with Studded Surfaces." Inst. Mech. Engrs.: 15-26.